# Title: Fitness adaptations of Japanese encephalitis virus in pigs following vector-free serial passaging

## Short title: Fitness adaptations of Japanese encephalitis virus in pigs

Andrea Marti[1-3], Alexander Nater[4], Jenny Pego Magalhaes[1,2], Lea Almeida[1,2], Marta Lewandowska[1-3], Matthias Liniger[1,2], Nicolas Ruggli[1,2], Llorenç Grau-Roma[2,5], Fadi Alnaji[6], Marco Vignuzzi[6,7], Obdulio García-Nicolás[1,2], Artur Summerfield[1,2] *

[1] Institute of Virology and Immunology IVI, Mittelhäusern, Switzerland.

[2] Department of Infectious Diseases and Pathobiology, Vetsuisse Faculty, University of Bern, Bern, Switzerland

[3] Graduate School for Cellular and Biomedical Sciences, University of Bern, Bern, Switzerland.

[4] Interfaculty Bioinformatics Unit (IBU) and Swiss Institute of Bioinformatics (SIB), University of Bern, Bern, Switzerland

[5] Institute of Animal Pathology, COMPATH, Department of Infectious Diseases and Pathobiology, Vetsuisse Faculty, University of Bern, Bern, Switzerland

[6] A*STAR Infectious Diseases Labs (A*STAR ID Labs), Agency for Science, Technology and Research (A*STAR), Singapore, Singapore

[7] Infectious Diseases Translational Research Programme, Department of Microbiology and Immunology, Yong Loo Lin School of Medicine, National University of Singapore, Singapore, Singapore

* Corresponding author

E-mail: artur.summerfield@unibe.ch (AS)

# Abstract

Japanese encephalitis virus (JEV) is a zoonotic mosquito-transmitted Flavivirus circulating in birds and pigs. In humans, JEV can cause severe viral encephalitis with high mortality. Considering that vector-free direct virus transmission was observed in pigs, JEV introduction into an immunologically naïve pig population could result in a series of direct transmissions disrupting the alternating host cycling between vertebrates and mosquitoes. To assess the potential consequences of such a realistic scenario, we passaged JEV ten times in pigs. This resulted in higher *in vivo* viral replication, increased shedding, and stronger innate immune responses in pigs. Nevertheless, the viral tissue tropism remained similar and frequency of direct transmission was not enhanced. Next generation sequencing showed single nucleotide deviations in 10% of the genome during passaging. In total, 25 point mutations were selected to reach a frequency of at least 35% in one of the passages. From these, six mutations resulted in amino acid changes located in the precursor of membrane, the envelope, the non-structural 3 and the non-structural 5 proteins. In a competition experiment with two lines of passaging, the mutation M374L in the envelope protein and N275D in the non-structural protein 5 showed a fitness advantage in pigs. Altogether, the interruption of the alternating host cycle of JEV caused a prominent selection of viral quasispecies as well as selection of de novo mutations associated with fitness gains in pigs, albeit without enhancing direct transmission frequency.

**Author summary:**

Japanese encephalitis virus (JEV) represents a major health threat in parts of Asia and Oceania. Primary vertebrate hosts are birds and pigs, but human infection also occurs and can cause severe encephalitis with high mortality. Like other Flaviviruses transmitted by insect bites, JEV requires replication in alternating cycles between mosquitoes on one side and birds or pigs on the other side. However, we previously reported that direct transmissions between pigs in absence of mosquitos can occur. Considering the increased

risks for such events after the spread of JEV to a new region with immunologically naïve pigs, the present study was performed to understand if and how a series of direct transmissions would promote JEV adaptations to pigs and change virus-host interactions. Pigs infected with JEV passaged ten times showed enhanced clinical symptoms and stronger antiviral immune response, but luckily no increase in direct transmission was observed. Nevertheless, genomic analysis demonstrated a complete change in dominant virus variants, as well as selection of six viral amino acid changes. This indicates that interruptions of the alternating lifestyle of JEV causes a strong evolutionary pressure, which through fitness adaptations can change the viral characteristics.

# Introduction

Japanese encephalitis virus (JEV) is a zoonotic mosquito-borne Flavivirus endemic in temperate and tropical regions of eastern and southern Asia as well as Oceania. JEV is the most common cause of viral encephalitis in humans, with a mortality rate of up to 30%. Survivors often suffer from neuropsychiatric sequelae [1–5]. The ecology of JEV is complex as it involves many vertebrates and is characterised by dual-host alternating cycling between mosquitoes and certain vertebrates requiring active replication in both hosts [6–8]. The main mosquito vector in Asia is *Culex tritaeniorhynchus* [9]. In vertebrates, a sufficiently high and long viremia is required to maintain the dual host cycling. Therefore, a prerequisite for this alternating host change is that Flaviviruses must be adapted to both hosts [10,11]. The main natural reservoirs of JEV are ardeid wading birds, but many different bird species develop viremia and seroconversion [12,13]. Importantly, JEV also infects a variety of mammals, such as humans, horses, dogs, ruminants, and pigs [14]. Amongst those, only pigs have been identified to be relevant in the ecology of JEV because they are highly susceptible to JEV infection and also develop high levels of viremia. Thereby, pigs serve as amplifying host for JEV, which is particularly critical considering that pigs are often kept in high density and proximity to humans [15].

In light of the above, the observation that JEV-infected pigs efficiently shed the virus through their oro-nasal fluids and that non-vector-borne direct transmission (DT) to naïve pigs occurs, represents a worrisome human and veterinary public health concern [16–18]. The impact of DT in the field is difficult to estimate. Mathematical modelling using longitudinal data from pigs in Cambodia supports a low rate of DT events between pigs in field conditions [19]. In JEV endemic areas, DTs are expected to be rare events, considering that a large percentage of pigs are serologically positive either by previous infection, vaccination or maternal antibodies [20,21]. However, this would be fundamentally different following JEV introduction into a new area with an immunologically naïve pig population. Such an event is not unrealistic considering the intense airway traffic, global trade and environmental changes introducing new animal species and vectors into certain regions [22,23]. In fact, in 2021/2022 JEV spread to Australia, infecting piggeries and leading to 46 human encephalitis cases and seven deaths [24].

Given this considerable public health threat, the present study was initiated to investigate possible consequences following several DT events in pigs. We hypothesised that the evolutionary pressure caused by a series of DT in pigs, together with the high mutation rate of RNA viruses, will alter virological characteristics that could impact virus-host interactions and transmission potential. To this end, we investigated changes in clinical parameters in organ tropism, duration and magnitude of viremia, antiviral and inflammatory response, oro-nasal virus shedding, and transmission. Furthermore, next-generation sequencing was employed to analyse changes in viral populations and mutational adaptation occurring during a series of vector-free infections in pigs.

# Material and Methods

## Ethics statement

All experiments were performed at biosafety level (BSL) 3 and approved following the Containment Ordinance (ESV SR 814.912) by the Swiss Federal Office for Public Health and

the Federal Office for the Environment (authorization number A110677-02). We also performed an internal risk-benefit evaluation (see S1 Methods). The experiments in pigs were conducted in compliance with the animal welfare regulation of Switzerland (TSchG SR 455; TSchV SR 455.1; TVV SR 455.163). The committee on animal experiments of the canton of Bern, Switzerland, reviewed the pig experimentation and pig blood collection protocols, and the cantonal veterinary authorities (Amt für Landwirtschaft und Natur LANAT, Veterinärdienst VeD, Bern, Switzerland) approved the animal experiments under the licenses BE101/19 and BE127/2020, respectively.

## Cells

*Aedes albopictus* C6/36 cells (ATCC) were cultured at 28°C and 5% $CO_2$. Vero cells (ATCC) and the porcine aortic endothelial cell line PEDSV.15 [25] (kindly provided by Dr. Seebach, University of Geneva, Switzerland) were cultured at 37°C and 5% $CO_2$. Porcine macrophages were derived from monocytes isolated from the blood of specific pathogen-free (SPF) Swiss Large White pigs as previously described [26]. Briefly, peripheral blood mononuclear cells were isolated by density centrifugation followed by monocytes purification using magnetic cell sorting. They were differentiated into macrophages and cultured at 39°C and 5% $CO_2$ [26]. Details of cell culture medium can be found in the S3 Methods.

## Virus stock

A genotype I-b JEV strain, originally isolated from a human patient in Laos in 2009 (JEV_CNS769_Laos_2009; kindly provided by Dr. Charrel, Aix-Marseille Université, Marseille, France) was used [27]. JEV stocks were produced using C6/36 cells infected with a multiplicity of infection (MOI) of 0.1 50% tissue culture infectious dose per cell ($TCID_{50}$/cell). After 72 hours post-infection (hpi) and culture at 28°C with 5% $CO_2$, the viral titres were determined as $TCID_{50}$ calculated according to the Reed-Muench formula [28]. The virus stocks were expanded three times on C6/36 cells before usage in this study as passage zero (P0).

## JEV Infection of pigs

Swiss Large White pigs from our SPF breeding facility were employed for all infection experiments. To model how a series of DT between pigs impacts JEV evolution, we performed a total of 10 passages (P) of JEV, employing a total of 30 pigs. Three pigs were infected oro-nasally with $10^5$ $TCID_{50}$/animal of JEV P0. Swabs and serum samples were taken at 0, 3 and 4 days post-infection (dpi). The day 4 serum was used for infection of three new pigs intranasally, keeping the lines separated (A, B and C). This was repeated until passage 10 (P10) was reached (Fig 1a). The clinical score (see S2 Methods) and the body temperature were measured daily. At 4 dpi of each passage, the pigs were euthanised by electrical stunning and exsanguination, and tissue samples from the mandibular lymph nodes, tonsils, thalamus, cortex and olfactory bulb were collected [29].

For the *in vivo* characterisation of P10, two groups of five pigs were infected oro-nasally with 1.8 x $10^5$ $TCID_{50}$/animal of either JEV P0 or P10. The latter represented a 1:1 mixture of P10 serum collected at 4 dpi from lines B and C. At 4 dpi, four naïve pigs were added to each group to evaluate DT rates. The infected pigs were euthanised at 11 dpi, while the in-contact pigs were kept until 15 dpi. Daily sampling of blood and swabs, as well as evaluation of clinical scores and body temperatures was performed by veterinarians participating in the blind trail. At 0, 3, 7 and 11 dpi, EDTA blood was collected. On the day of euthanasia, tissue samples were collected as described above (Fig 3a).

## RT-qPCR

Viral RNA was extracted using the NucleoMag VET kit (Macherey Nagel) and the extraction robot Kingfisher Flex (Thermo Fisher). Viral RNA was quantified by RT-qPCR with the AgPath-ID One Step RT-PCR KIT (Thermo Fisher), using the forward primer 5' - ATC TGA CAA CGG AAG GTG GG – 3', the reverse primer 5'-TGG CCT GAC GTT GGT CTT TC - 3' and the probe 5' – FAM - AGG TCC CTG CTC ACC GGA AGT – TAMRA -3'. Viral genomic RNA was quantified relative to a T7 *in vitro* transcribed reference JEV RNA (473 bases long

sequence within the 3'-untranslated regions (UTRs) of JEV Laos), which was used as a standard (S4 Methods). For the standard curve, a dilution series spanning the range of $10^7$ to $10^1$ copies/µl was used. The detection cut-off was defined at $10^1$ copies/µl. Samples were analysed using a 7500 Applied Biosystems real-time PCR machine (Thermo Fisher).

## Transcriptomics

Transcriptomic analyses employed RNA extracted from blood leukocytes as described in the S5 Methods. Libraries were prepared using the BRB-seq Library preparation kits (Alithea, Switzerland) at the Next Generation Sequencing (NGS) Platform of the University of Bern. Quality control employed a 5200 Fragment Analyzer CE instrument (Agilent), and sequencing the Illumina® NovaSeq6000 sequencer. Reads were mapped to the pig genome (*Sus scrofa* 11.1, Ensembl release) using Tophat v.2.0.11 [30–33]. The number of reads overlapping with each gene was evaluated with Htseq-count v.0.6.1 [34,35]. The Bioconductor package DESeq2 v1.38.3 [36] was used to test for differential gene expression between the experimental groups. Gene set enrichment analysis (GSEA) was performed following ranking of genes based on differential gene expression using the "stat" value [37,38]. Calculations of normalized enrichment scores and false discovery rates (FDR) were performed using online tools available on https://www.gsea-msigdb.org [39]. Blood transcriptional modules (BTM) defined by Li et al. [40] for humans and modified for pigs [41] were used. Figures were created in R 4.3.0 using the ggplot2 package.

## Pathology

For tissue preparation and pathological assessment please read the S6 Methods.

## Serum neutralisation assay

Serum neutralization assays were performed by adding serially diluted sera and 100 focus forming units of JEV per well using Vero cells. After incubation for 48h, the cells were stained for viral E protein to determine the 50% neutralizing dose ($ND_{50}$) of the sera. Details of the protocol are described in the S7 Methods.

## Growth curves of passaged viruses

Confluent C6/36 and PEDSV.15 cells were infected with JEV isolated from sera (see S8 Methods) at an MOI of 0.01 $TCID_{50}$/cell. After 1.5h of incubation, the inoculum was removed, the cells were washed twice with pre-warmed PBS, and fresh medium was added. The time point 0 hpi was harvested right after washing. The supernatant was further harvested at 18, 24, 48 and 72 hpi, and analysed by RT-qPCR, and viral titrations on C6/36 and PEDSV.15 cells. For the titration of JEV from cell culture supernatants, the cells were seeded in a 96-well plate. Once cell confluency was reached, the medium was replaced. Then, virus samples were ten-fold serially diluted, starting at 1:10 dilution in quadruplicates and incubated for three days. The cells were washed with PBS and fixed with 4% formalin. Finally, virus-infected cells were labelled by an immunoperoxidase-staining as described in the S7 Methods and $TCID_{50}$/ml was determined [28].

## Cytokine quantification

Interferon gamma (IFN-γ), interleukin 1 alpha (IL-1α), IL-1β, IL-1ra, IL-2, IL-4, IL-6, IL-8, IL-10, IL-12, IL-18 and tumour necrosis factor (TNF) levels in serum samples of the infected pigs at -3, 3, 4, 5 and 7 dpi were quantified using the Milliplex MAP Porcine Cytokine/ Chemokine Magnetic bead kit (Millipore) and the BioPlex Magpix Reader (Bio-Rad). IFN-α was measured in duplicates by ELISA as previously described [42].

## Viral genome analyses

For the viral genome sequencing, RNA was extracted from serum or swab samples. For details on extraction, RNA quality and quantity evaluation, library preparations we refer to the S9 Methods. Libraries were sequenced at 100 bp paired-end using an Illumina NovaSeq 6000 S4 Reagent Kit v1.5 (200 cycles; Illumina) on an Illumina NovaSeq 6000 instrument. The quality of the sequencing run was assessed using Illumina Sequencing Analysis Viewer (Illumina version 2.4.7) and all base call files were demultiplexed and converted into FASTQ files using Illumina bcl2fastq conversion software v2.20. Quality control of raw sequencing

reads used FastQC v0.11.9 [43]. Removal of adapter sequences and extraction of unique molecular identifiers (UMIs) were performed with Fastp v0.23.4 [44]. We classified read pairs using Kraken2 v2.1.2 [45] by exact k-mer matching to a custom database consisting of multiple host and potential contaminant genomes, including GRCh38 (Homo sapiens), Sscrofa11.1 (*Sus scrofa*), GCF_006496715.1 (*Aedes albopictus*), and GCF_001876365.2 (C6/36), as well as JEV sequences KY927816, KC196115, and EF571853. We extracted all read pairs classified as being derived from JEV Laos for further analysis.

A *de novo* reference sequence of JEV Laos strain was assembled from pre-processed and filtered reads of the P0 sample using SPaDES v3.15.5 [46] in the 'rnaviral' mode. The resulting reference genome was manually curated and a GTF file of gene annotations was created based on alignments of protein-coding sequences to the assembled genome. Reads were mapped to the reference genome using BWA mem v0.7.17 [47] and SAM files were converted to BAM format with SAMtools v1.17 [48]. UMI sequences were moved from read names to a tag in the BAM files using the CopyUmiFromReadName command of fgbio v2.1.0 [49]. Run-wise BAM files were then merged for each sample and deduplicated using the MarkDuplicates tool of GATK v4.4.0.0 [50]. Based on the resulting duplicate-marked BAM files, single-nucleotide variants were called per sample using LoFreq v2.1.5 [51] without applying default filters for coverage or strand bias. Genome-wide mapping statistics were obtained with the flagstat command of SAMtools v1.17 [48] and Mosdepth v0.3.3 [52]. Analysis of the site-wise sequencing depth for each sample was performed with the depth command of SAMtools v1.17 [48]. Variant effects and sequence statistics were calculated with SNPGenie v1.0 [53]. Allele frequency trajectories and genetic diversity statistics along the passages were generated with custom Python scripts using the sample-wise VCF files and filtering for a minimum site-wise sequencing depth of 100 based on the output of SAMtools depth. Networks of pairwise allele frequency correlations between variant sites across passages were generated with Cytoscape v3.10.1 [54]. All statistical analyses were run in R version 4.2.1 (2022-06-23) [55].

### Statistical Analysis

Statistical analyses of the non-bioinformatical datasets were performed with GraphPad Prism 8.0 (GraphPad Software, La Jolla, USA). The analyses related to the *in vivo* passaging and the *in vivo* characterization were performed using a non-parametric, two-tailed Mann-Whitney U-test. The *in vitro* growth curves were analysed by Tukey's multiple comparison test (ANOVA). The significance level was determined by p values with *p<0.05, **p<0.01; ***p<0.001; **** p<0.0001. p values above 0.05 were considered non-significant.

# Results

### Serial passaging of JEV in pigs

To identify virus adaptations associated with a series of direct transmissions of JEV in pigs, a total of 10 passages were performed in three independent sets of pigs (line A-C) as depicted in Fig 1a. The passaging was performed blindly, not checking the viral loads in the animals. During passaging, the infectivity was lost at P5 in line A. Therefore, there is no line A data for P5-P10 in Fig 1 and 2. Most infected pigs had increased body temperatures and clinical scores at 3 and/or 4 dpi (Fig 1b, c). The piglets showed reduced liveliness and appetite during the peak of infection. A statistical comparison of P0 with the later passages using the combined data at 3 and 4 dpi indicated reduced fever during P4, P5, P8 and P10 and reduced clinical signs for P4, P5, P6, P7 and P9. All infected pigs were viremic at 3 and 4 dpi, with $10^4$ to $10^5$ viral copies/µl serum (Fig 1d). Although viremia levels did not change significantly over the passages, viral RNA loads in oro-nasal swabs were significantly higher in P7, P9 and P10 when compared to earlier passages, increasing from $10^1$ to $10^3$ viral copies/µl (Fig 1e). The viral RNA loads in central nervous and lymphoid tissues collected at 4 dpi did not show significant differences between the passages (S1 Fig). It is important to note that clinical differences may also have been influenced by age effects. The pigs used for the data shown in Fig 1 and 2 were from different litters. Therefore, not all animals had the same

age at the day of infection. For these reasons we further characterized the viruses isolated from P1-P10.

## Passaged JEV did not result in enhanced fitness *in vitro* in porcine cells

To identify possible changes in replication characteristics, we performed comparative growth curves in insect C6/36 and porcine PEDSV.15 cells. The analysed viruses included JEV P0 (stock used to infect the first passage in pigs), P1, P5 and P10. With C6/36 cells, both lines of P1, P5 and P10 viruses demonstrated a clear delay in replication compared to P0, particularly visible at the 24 hpi. This observation was made at both viral RNA and progeny virus level, independently of the cell type used for titration (Fig 2a). To evaluate if this apparent loss of fitness in insect cells is also observed in porcine cells, we performed identical growth curves using PEDSV.15 cells (Fig 2b). Interestingly, viral RNA loads were not significantly different between P0 and P1, P5 and P10, except for 18hpi. Nevertheless, P0 virus outgrew the passaged JEV in terms of viral titres determined in PEDSV.15 cells at 48 and 72 hpi. This was also observed for line C viruses when titrations used C6/36 cells. These data indicate that all viruses isolated from pigs had delayed and reduced *in vitro* replication characteristics compared to P0 JEV**.**

As all serum viruses were rescued on macrophages, while the P0 working stock came from C6/36, the measured growth kinetics were additionally statistically analysed, comparing P1 with P5 and P10. Interestingly, this analysis identified enhanced fitness of P10 (and sometimes also P5) in line C when grown on C6/36 cells. At 48-72 hpi higher titres were observed independent of the cell type used for titration (Fig 2a). Surprisingly, this enhanced fitness was not observed with the growth curves in PEDSV.15 cells (Fig 2b) and neither in the growth curves of line B.

## Passaged JEV increased viremia, nasal shedding and clinical symptoms

To identify if a series of direct transmissions modelled by passaging the virus in pigs could result in possible changes in virulence, organ tropism, virus shedding and direct transmission

283 capacities, we infected five pigs with either JEV Laos P0 or a 1:1 mix of pig serum P10B and
284 P10C (Fig 3a). The P0 infected groups are stated as Passage 1* (P1*), to differentiate from
285 the passage 1 of the previous animal experiment, while the P10 infected pigs are termed as
286 passage 11 (P11). For both groups, the clinical, virological, pathological and immunological
287 parameters were assessed (Fig 3, 4 and 5). In addition, at 4 dpi four naïve pigs were co-
288 housed to obtain information on possible changes in direct transmissibility (Fig 6). The
289 infected pigs were euthanised at 11 dpi, while the in-contact pigs were kept until 15 dpi.

290 When comparing the P11 to P1*, the P11 pigs showed a similar course of disease, but with
291 signs of enhanced virulence (Fig 3b-h). With P11 we observed a significantly increased body
292 temperature at 3, 4 and 8 dpi (Fig 3b), higher clinical scores at 3 and 7 dpi (Fig 3c), higher
293 viremia at 3 dpi (Fig 3d), higher viral RNA loads in nasal swabs at 8 dpi (Fig 3e) and higher
294 viral loads in the thalamus at 11 dpi (Fig 3g). The enhanced clinical scores and nasal
295 shedding were confirmed by area under the curve analyses (Fig 3c, e).

296 After euthanasia, JEV RNA was identified in the cortex, thalamus, olfactory bulb, tonsils and
297 mandibular lymph nodes with the highest levels in the tonsils (Fig 3g). This was similar
298 between P1* and P11 groups and was consistent with previous observations [17,29,56]. All
299 infected pigs showed mild to moderate histopathological lesions in the CNS without group
300 differences in the infected pigs (Fig 2h and S2 Fig) indicating that organ tropism and neuro-
301 invasiveness of JEV was not affected by the passaging. No lesions were observed in the
302 tonsils and mandibular lymph nodes.

303 **Passaged JEV stimulated stronger innate immune responses**

304 Considering that no information on *in vivo* cytokine responses in pigs were available, and
305 that a series of vector-free direct transmission in pigs could also impact how JEV interacts
306 with the host immune system, we investigated the innate and adaptive immune responses in
307 serum samples from the experiment described in Fig 3a. Following infection with both
308 viruses, increased levels of IL-12, IL-6, IFN-α and IL-1RA were found between 3-7 dpi (Fig
309 4a-d). Other cytokines, including IL-1α, IL-2, IL-10 and IL-18, were significantly elevated only

310 at individual days and not with both viruses (Fig 4e-h). GM-CSF, IL-4, IL-1β, TNFα and IL-8
311 were not induced systemically by JEV (S3 Fig). Altogether, this cytokine profile indicates that
312 JEV induces a Th1 and antiviral response in which proinflammatory responses are well-
313 controlled. When comparing the P1* and P11 groups, we found increased early IFN-α and
314 anti-inflammatory IL-1RA responses in the P11 pigs (Fig 4c, d).

315 Independently of the infected group, antibody neutralising titres were detected as early as 5
316 dpi, reaching very high titres at 9 dpi (Fig 4i). This kinetic appeared to coincide with control of
317 viremia (see Fig 3d).

318 To further elaborate on innate immune responses induced by JEV, and on how passaging
319 would impact such responses, we performed a transcriptome analysis of blood leukocytes
320 before infection and at 3, 7 and 11 dpi from the P1* and P11 groups. We employed GSEA
321 analyses with porcine BTM as gene modules, which have been demonstrated to provide
322 comprehensive immunological information following virus infection [41,57,58]. BTM related to
323 the innate immune system were grouped in antiviral, dendritic cell (DC), inflammation,
324 myeloid and NK cell BTM families (Fig 5a, b). In both groups, JEV induced the expected
325 antiviral response at 3 dpi, which was followed by an enhancement of the NK cell BTM at 7
326 and 11 dpi. While JEV infection decreased expression of many DC, inflammation and
327 myeloid cells at three days post-infection in the P1* group, this was not observed for P11,
328 which increased expression of a few of these BTM such as M165, M67, S11 (all activated
329 DC), as well as M86.0, M27.0 (chemokines and inflammatory mediators). Nevertheless, at 7
330 and 11 dpi, both groups showed a similar prominent downregulation of DC, inflammation and
331 myeloid cell BTM, possibly related to the anti-inflammatory cytokine responses (Fig 4).

332 To investigate group differences in more detail, the transcriptome profiling on each day was
333 compared between the groups (Fig 5b). This clearly confirmed that early innate immune
334 responses were stronger following infection in the P11 pigs. More specifically, seven antiviral
335 BTM, 11 BTM related to DC, 16 BTM related to inflammation, 13 myeloid cell BTM and one
336 NK cell BTM were higher in the P11 compared to the P1* group. In a later stage of the

337 infection (7 dpi) immunoregulatory mechanisms leading to a downregulation of certain of the
338 innate BTM were more pronounced with P11 compared to P1* (Fig 5b).

339 We next investigated BTM related to the adaptive immune system. These were further
340 classified as “B-cells”, “cell cycle”, and “T-cells” BTM (Fig 5c, d). Overall, the pattern of BTM
341 induced in the two groups looked similar (Fig 5c). Both viruses induced a plasma cell
342 response (M156.1) at 7 dpi, whereas all other BTM were downregulated. In contrast, cell
343 cycle BTM were mostly induced, in particular at 7 dpi. Similarly, T cell BTM were also
344 strongly induced at all days for the P1* pigs and at 7 and 11 dpi for the P11 pigs (Fig 5c).
345 Comparison of the groups at individual dpi did not reveal many differences in the BTM
346 expressions but confirmed a higher T-cell activation in the blood of the P1* (Fig 5d).

347 Taking together, JEV induced an antiviral and Th1 immune response accompanied by a
348 potent neutralising antibody response and an anti-inflammatory regulation. The higher innate
349 immune responses found after infection with passaged JEV are possibly a consequence of
350 increased virus replication rates. Our data indicate also that there was no acquisition of
351 improved immune evasion capacities because of passaging.

352 **Passaged JEV showed no increased vector-free transmissibility**

353 To determine possible changes in direct transmission, four in-contact animals were added to
354 each group of the oro-nasally infected pigs. As shown in Fig 6, only one in-contact sentinel
355 pig was infected in the P1* group. In this animal, the kinetics of JEV in serum and swab
356 samples were similar to that seen with oro-nasally infected animals (Fig 6a, b). This pig was
357 also the only sentinel pig that developed neutralising antibodies (Fig 6c) and showed
358 histological lesions in the brain (Fig 6d).

359 **25 single-nucleotide deviations were positively selected**

360 Taking all P0-P10 viruses into consideration, single-nucleotide variations in 10% of the JEV
361 genome locations were observed (Fig 7a). In P0, 220 nucleotide deviations from the
362 consensus Laos sequence were found. During passaging, additional 8% of the nucleotide

363 positions mutated. The nucleotide deviations were distributed throughout the viral genome,
364 with being 33% synonymous and 58% non-synonymous changes. 2% of the mutations led to
365 stop codons and 8% were located in the UTRs (Fig 7a, S1 Table). To focus on positively
366 selected nucleotide deviations, we filtered for a frequency above 35% in at least one line and
367 passage. This identified 25 single-nucleotide deviations, three in the UTRs, 16 synonymous
368 and six non-synonymous. From the latter, two amino acid changes were in the envelope (E),
369 two in the non-structural protein 5 (NS5), one in the precursor of the membrane (prM) and
370 one in the non-structural protein 3 (NS3).

371 To determine changes in genetic variability, we calculated the nucleotide diversity (π) for
372 each sample of the three lines. π represents the average number of nucleotide differences
373 per site between two viral haplotypes randomly chosen from the viral quasispecies
374 populations. As shown in Fig 7b, π increased from P0 to P1 possibly pointing on an initial
375 diversifying selection at the expense of dominant populations present in P0. Between P1 and
376 P10 π remained at a stable level indicating a balance between mutational diversification and
377 selection processes.

378 As a measure of differentiation of viral populations along the passaging, we calculated the
379 Fixation Index $F_{ST}$, based on the pairwise variance in allele frequencies between P0 and the
380 passaged viral populations. Zero indicates no genetic differentiation between P0 and the
381 passage of interest, while 1 indicates complete differentiation. As expected, an increase of
382 $F_{ST}$ over time was observable for all three lines during passaging (Fig 7c). Temporary
383 increases in $F_{ST}$ were observed in lines A (P3) and line C (P8) and associated with reduced
384 π values (Fig 7 b, c). The data also indicates that in line C, more prominent population
385 differentiations were observed compared to line B. We also calculated the π and the $F_{ST}$ for
386 each protein and the UTRs separately (S4 Fig and S2 Table). As expected, the π profiles of
387 individual viral genes were mostly comparable to those of the whole genomes. One
388 exception was the NS4B, which had already a high diversity in P0 that was not further

389 enhanced during passaging. For $F_{ST}$, most viral genes had unique profiles indicating
390 selection of mutations present on individual genes.

391 **Trajectory analyses identifies JEV variants with fitness gain in pigs**

392 We next made trajectory analyses for the 25 single-nucleotide variants that reached at least
393 a frequency 35% once during passaging. Some of these single-nucleotide deviations
394 followed quasi-identical trajectories along the passages indicating their localization on the
395 same viral RNA molecule (Fig 8a). Based on this feature, we defined viral haplotypes when
396 the frequencies of at least two nucleotide deviations were quasi-identical over the passages
397 (Cosine similarity > 0.999 between the frequencies trajectories of single-nucleotide
398 deviations in the haplotype). Of note, due to the short-read sequencing, a final proof for
399 haplotypes is missing. However, the very similar frequencies suggest that these haplotypes
400 were most likely co-inherited and therefore present on a single viral genome.

401 Haplotypes 1 and 3 were present at high frequency in P0 (20% and 28%, respectively) but
402 were de-selected in the surviving lines after 2-5 passages. In line A, haplotype 3 reached
403 >97% frequency by P3, before this line became extinct after P4 (Fig 8a). Three mutations
404 from haplotype 2b (4062, 5778 and 8500) were also detectable in P0 at frequencies of
405 around 3%, and were selected to over 95% in lines B and C. In haplotype 2a, a mutation at
406 position 4539 evolved at P2 in line B only. The remaining haplotypes 4-7 were not detectable
407 in P0 and we cannot determine if these were selected from pre-existing minor variants in P0
408 or evolved by simultaneous mutations on one strand of the viral genome. Haplotype 4 only
409 arose in line C and reached >95% frequency. Haplotypes 5 and 6 arose in P1 of only one
410 line (C and B, respectively) and disappeared after initial selection. Finally, haplotype 7 was
411 detectable only after 5-7 passages in line B, indicating that it probably emerged by
412 simultaneous mutations on two sites of one genome. In addition to the above haplotypes, a
413 total of five individual mutations were selected to reach levels over 35% (Fig 8b and S1
414 Table).

## Competitive advantage for haplotype 2, haplotype 7 and mutations at positions 4539, 7548 and 10557

To determine fitness differences in haplotypes and mutations present in lines B and C, we also sequenced the viruses obtained from the comparative P0/P10 pig infection experiment, in which the P10 inoculum represented a 1:1 mixture of lines B and C. These viruses obtained from a total of five pigs were termed P11. The only single-nucleotide variants staying at 100% were those of haplotype 2b. Haplotype 7 (2098 and 8283 mutations in line B) showed a relative increase, while haplotype 4 (mutations 429, 1077 and 8922 in line C) showed a relative decrease in frequencies (Fig 9a and S1 Table). A positive selection was also observed for mutations 4539, 7548 and 10557 emerging in line B. Surprisingly, only two emerging mutations that caused amino acid changes showed a fitness advantage in this experiment. One was in haplotype 7 at position 2098 encoding the E protein (Met→Leu), and the other in haplotype 2 at position 8500 encoding the NS5 (Asn→Asp). Interestingly, the animal in which these line B haplotype/mutations were mostly selected also had the highest viremia and IFN-$\alpha$ levels (square symbol in Fig 3, 4 and 9).

## Passaging of JEV in pigs results in prominent selections of pre-existing variants to change the overall quasispecies composition

Fig 9b visualizes the evolution of divergent nucleotides that were already present in P0. Many of these variants were still present at comparable frequencies in P1* but not P11. In all pigs, the dominant quasispecies had dramatically changed. Dominant variants with frequencies >5% in P0 were mostly undetectable in P11 at the expense of minor variant amplification (Fig 9b and S1 Table). This indicates that a series of direct transmission events in pigs is associated with strong selection and de-selection processes of pre-existing minor variants.

# Discussion

Mosquito-borne Flaviviruses have evolved by adaptation to both insects and vertebrates to maintain an alternating host cycle. The clear genetic, physiological and immunological differences between insects and vertebrates requires viral adaptation, processes that may involve fitness trade-offs in both or in one of the hosts [59]. The high mutational frequency of Flaviviruses in the range of $10^{-3}$ to $10^{-5}$ per replicated nucleotide creates a swarm of mutants which enables the selection of pre-existing quasispecies, as well as the continued selection of mutations to ensure fitness in the current host [60]. It should be noted that trade-offs following adaptation to one host have not always been observed with Flaviviruses [61]. Furthermore, despite the relatively wide host plasticity of many vector-borne viruses, Flaviviruses have adapted to efficiently replicate in rather selective vertebrate hosts, for JEV being birds and pigs.

Given the ability of JEV to transmit directly between pigs in contact [17], a series of vector-free transmission events would be possible after introduction of JEV into a herd of immunologically naïve pigs. Hence, the present study addressed whether and how such an event could alter virus pathogenesis and viral genetic features. Our data demonstrate that JEV passaging in pigs induced virus adaptations associated with enhanced viremia, nasal shedding, clinical scores and innate immune responses. This can be interpreted as an increase in viral fitness and relates to previous observations found with other Flaviviruses following passaging in vertebrates such as West Nile virus (WNV) in chicks [62], Zika virus (ZIKV) in mice [63–65] and also JEV in mice [66]. However, JEV passaging in suckling mice was also reported to result in attenuation [67]. Nevertheless, considering that mice are not a natural host of ZIKV or JEV, the evolutionary pressure on the virus during experimental passaging is expected to be quite different.

Despite the fitness gain observed in the present study, the fundamental characteristics of the infection as well as the transmission rate remained similar. The latter was unexpected

considering that the longer nasal shedding should favour direct transmission. In fact, viral doses as low as 10 $TCID_{50}$ applied via the oro-nasal route to pigs were found to produce a JEV infection [17]. A possible explanation could be that the stronger clinical symptoms in the P10-infected pigs reduced the contact between animals. Our transmission data combined with our previous observations confirms the possibility of direct transmission between pigs, but also indicate that these may be relatively rare events requiring intensive contact between pigs. Nevertheless, it should be noted that our pigs were kept at a low stock density (>3 $m^2$ per animal). Commercial farming uses 0.7-1 $m^2$ of space per pig, depending on the country [68–70]. It is conceivable that under dense commercial farming condition direct transmission events could be favoured [71,72]. It is also possible that direct transmission is influenced by the viral strain. These aspects are relevant and require further investigations considering that during the recent outbreak of JEV in Australia in 2021/2022 over 80 piggeries were affected [73]. Interestingly, this outbreak was caused by a recently emerged genotype IV virus [74], which had a high mutation rate, possibly enabling a fast virus evolution and adaptation [75]. To our knowledge it is not known whether direct transmission events between pigs took place in Australia and whether the characteristics of the virus changed during the epidemic. We recommend that this should be investigated.

We also aimed to identify a possible change of the *in vitro* phenotype caused by the *in vivo* passaging by comparing the viral growth kinetics in insect and porcine cells. The comparison of P0 with P10 demonstrated much faster growth of P0, which pointed to a cell culture adaptation phenomenon. Indeed, P0 had been cultured for three passages to create the master and working stock termed “P0”. Rapid cell culture adaptation effects are well-known for many viruses. For instance, only three *in vitro* passages of WNV increase replication characteristics [76]. For JEV, five passages in cell culture resulted in increased glycosaminoglycan receptor binding [77,78]. Therefore, we also compared the growth kinetics of JEV from P1, P5 and P10, which were all isolated by antibody-dependent enhancement on macrophages. Also, this comparison did not reveal the expected adaptation

to porcine cells, indicating that our *in vitro* models may not be suitable to address species adaptations associated with fitness changes.

After only one passage we found a jump in genetic diversity indicating a rapid replacement of dominant populations present in P0 by minority variants. One could speculate that this effect may be related to a dramatic reduction in cell-culture adapted variants explaining the delayed *in vitro* replication of pig-passaged JEV. Nevertheless, no prominent mutation on the E protein was identified that could have explained this effect. Therefore, it could simply be related to the rapid ability of Flaviviruses to recover lost diversity following bottleneck effects (in this case the cell culture) [59].

Interestingly, from P1 to P10 the genetic diversity was stable indicating a balance between mutational diversification and selection processes. This observation may relate to the fact that JEV is well-adapted to pigs. However, $F_{ST}$ steadily increased until P5-6 pointing to selection of existing variants and/or new mutations. To investigate this in detail, we analysed the trajectories of all nucleotide variations reaching at least a frequency of 35% during the passages. Some of these mutations were classified as belonging to seven different haplotypes that contained at least two mutations with quasi-identical frequencies over the passages and were therefore most likely present on a single viral genome. Some of these haplotypes were already detected in the P0 swarm and were therefore clearly selected or deselected during passages. In particular haplotype 2a and 2b have increased fitness in pigs as they were selected in the two surviving lines B and C. In contrast, haplotype 3 was selected only in line A and reached nearly 100% before extinction of this line at P4. Of note, this haplotype as well as haplotype 4 did not contain mutations resulting in amino acid changes indicating the importance of other elements such as RNA secondary structures or codon optimization during selection.

As haplotypes 4-7 were not detected in P0, we cannot definitively conclude if they represent rare minor variants or if they were generated by simultaneous mutations on one genome. Most likely, haplotype 7 emerged by mutations as it was first detected after P5. In addition to

519 haplotype 7, five single mutations arose during passaging. This is in line with the fact that
520 random mutations will in most cases be deleterious for a virus [60].

521 Overall, six nucleotide deviations led to amino acid changes. In line C, we found a mutation
522 within prM at position 515 of the genome, in which a polar threonine was replaced by a non-
523 polar isoleucine (prM T13I). This was not described in a published JEV genome so far,
524 although this position is not particularly conserved between different Flaviviruses [79].
525 Studies on ZIKV and JEV showed that point mutations in the prM protein can alter the
526 infectivity of the virus [80–82]. It should be noted that in the competition experiment with the
527 simultaneous infection with line B and C, prM T13I had a reduced frequency.

528 Only two amino acid changes were found in the E protein at positions 2074 (amino acid (AA)
529 position 366) and 2098 (AA374). The S366P change was on haplotype 1, which was de-
530 selected. M374L is more interesting as it emerged only at P7 in line B, and was positively
531 selected in the competition experiment. We were only able to find 374L in West Nile viruses
532 [83,84]. It is located in the DIII domain of the E protein, which is partly exposed and targeted
533 by antibodies. Interestingly, AA374 is the only variable position in this conserved domain
534 (AA373-379) [85].

535 An amino acid change in the genomic position 6356 was localized in the NS3 protein at
536 AA583 changing valine to alanine. This change was only selected in P1 of line B and then
537 de-selected. 583A was not present in any of the JEV sequence data published on NCBI but
538 found to be variable when comparing different Flaviviruses. While Dengue viruses and Zika
539 viruses often harbour a tryptophan, Usutu virus has a valine and Saint Louis encephalitis
540 virus a phenylalanine at this position [86–89]. In fact, the 583 position does not localize to the
541 conserved RNA helicase domain [90,91].

542 At the genomic position 8500 within the NS5 gene, the amino acid change N275D was
543 strongly selected in the pre-existing haplotypes 2a and 2b in lines B and C. N275D was
544 described in two JEV isolates (GenBank: MH753129.1, JN381843.1) and other Flaviviruses
545 like West Nile virus, yellow fever virus, Yokose virus and Murray valley encephalitis virus

546 [92–94]. AA275 is located in a linker site between the functional domains of the RNA-
547 dependent RNA polymerase and the methyltransferase [94]. The linker spans the amino
548 acids 266 to 275 and shows little conservations between Flaviviruses. Removal of the linker
549 does not abrogate polymerase activity [95]. Since the N275D variant was efficiently selected
550 in both lines in pigs, it would be interesting to investigate this position in future studies.

551 The final amino acid change was caused by a mutation at genomic position 9658 first
552 detected in P7 of line B. It resulted in a change of threonine to alanine in the NS5 protein
553 (T661A), previously found in JEV (GenBank AB830335), replacing a polar with a non-polar
554 amino acid at the end of a predicted alpha helix. While threonine can bend the alpha helix,
555 alanine represents a stabilizing amino acid [96]. The alpha helix flanks a conserved motif of
556 the NS5 protein [97]. The aspartate residues 667 and 668 of this conserved motif are
557 hypothesized to play a role in the regulation of magnesium cations during the polymerization
558 [98]. Although T661A was selected in line B it did not have a competitive advantage in the
559 lines B/C co-infection.

560 Taken together, passaging JEV in pigs to mimic a series of direct transmission can increase
561 its fitness in pigs in terms of higher viremia and increased mucosal shedding. Nevertheless,
562 the pig's immune system remains effective in controlling the infection and the overall disease
563 characteristics remain similar. Passaging is associated with both a dominant selection of pre-
564 existing haplotypes as well as *de novo* mutations. Despite these strong selection processes
565 the overall genetic diversity is maintained during passaging. Studies are ongoing to
566 determine if the described viral adaptation results in a loss of fitness in mosquitoes. Our work
567 contributes to understanding how Flaviviruses maintain fitness after interruption of alternating
568 host cycling. Despite strong genetic selection processes following passaging in pigs, the
569 impact on disease progression, viral tropism and immune response characteristics were
570 limited, pointing to a high level of JEV adaptation to the pig host. Fortunately, JEV did not
571 appear to adapt for increased direct transmission.

# Acknowledgements

We thank Katarzyna Sliz and Daniel Brechbühl for the animal care during the experiments and Urs Pauli and Ruth Knorr for the support regarding biosafety. We are grateful to Razieh Ardali for her support in the analysis of the transcriptomic data and Francisco Brito for help with the preparation of Fig 9b. We greatly appreciated all the help and work of Pamela Nicholson, Daniela Steiner and Samia Imadjane from the Next Generation Sequencing Platform (University of Bern, Bern, Switzerland) for the BRB-sequencing and the total RNA-sequencing. We thank Remi Charrel and Antoine Nougairede (Aix-Marseille Université, Marseille, France) for providing the JEV strain Laos and Dr. Jörg Seebach (University of Geneva, Switzerland) for the PEDSV.15 cell line.

# References

1. Turtle L, Solomon T. Japanese encephalitis — the prospects for new treatments. Nat Rev Neurol. 2018;14: 298–313. doi:10.1038/nrneurol.2018.30

2. Weaver SC, Barrett ADT. Transmission cycles, host range, evolution and emergence of arboviral disease. Nat Rev Microbiol. 2004;2: 789–801. doi:10.1038/nrmicro1006

3. Campbell G, Hills S, Fischer M, Jacobson J, Hoke C, Hombach J, et al. Estimated global incidence of Japanese encephalitis: Bull World Health Org. 2011;89: 766–774. doi:10.2471/BLT.10.085233

4. World Health Organization. Japanese encephalitis. In: WHO.int [Internet]. 9 May 2019 [cited 27 Jul 2023]. Available: https://www.who.int/news-room/fact-sheets/detail/japanese-encephalitis

5. van den Hurk AF, Ritchie SA, Mackenzie JS. Ecology and Geographical Expansion of Japanese Encephalitis Virus. Annu Rev Entomol. 2009;54: 17–35. doi:10.1146/annurev.ento.54.110807.090510

6. Franz A, Kantor A, Passarelli A, Clem R. Tissue Barriers to Arbovirus Infection in Mosquitoes. Viruses. 2015;7: 3741–3767. doi:10.3390/v7072795

7. Van Den Eynde C, Sohier C, Matthijs S, De Regge N. Japanese Encephalitis Virus Interaction with Mosquitoes: A Review of Vector Competence, Vector Capacity and Mosquito Immunity. Pathogens. 2022;11: 317. doi:10.3390/pathogens11030317

8. Mellor PS. Replication of Arboviruses in Insect Vectors. Journal of Comparative Pathology. 2000;123: 231–247. doi:10.1053/jcpa.2000.0434

9. Le Flohic G, Porphyre V, Barbazan P, Gonzalez J-P. Review of Climate, Landscape, and Viral Genetics as Drivers of the Japanese Encephalitis Virus Ecology. Johansson MA, editor. PLoS Negl Trop Dis. 2013;7: e2208. doi:10.1371/journal.pntd.0002208

10. Park SL, Huang Y-JS, Vanlandingham DL. Re-Examining the Importance of Pigs in the Transmission of Japanese Encephalitis Virus. Pathogens. 2022;11: 575. doi:10.3390/pathogens11050575

11. Zhang Y, Liang D, Yuan F, Yan Y, Wang Z, Liu P, et al. Replication is the key barrier during the dual-host adaptation of mosquito-borne flaviviruses. Proc Natl Acad Sci USA. 2022;119: e2110491119. doi:10.1073/pnas.2110491119

12. Hameed M, Wahaab A, Nawaz M, Khan S, Nazir J, Liu K, et al. Potential Role of Birds in Japanese Encephalitis Virus Zoonotic Transmission and Genotype Shift. Viruses. 2021;13: 357. doi:10.3390/v13030357

615 13. Page MJ, Cleton NB, Bowen RA, Bosco-Lauth A. Age-Related Susceptibility to
616 Japanese Encephalitis Virus in Domestic Ducklings and Chicks. The American Journal
617 of Tropical Medicine and Hygiene. 2014;90: 242–246. doi:10.4269/ajtmh.13-0161

618 14. Mansfield KL, Hernández-Triana LM, Banyard AC, Fooks AR, Johnson N. Japanese
619 encephalitis virus infection, diagnosis and control in domestic animals. Veterinary
620 Microbiology. 2017;201: 85–92. doi:10.1016/j.vetmic.2017.01.014

621 15. Gresser I, Izumi T, Moyer JT, Scherer WF, McCown J. Ecologic Studies of Japanese
622 Encephalitis Virus in Japan: VI. Swine Infection*. The American Journal of Tropical
623 Medicine and Hygiene. 1959;8: 698–706. doi:10.4269/ajtmh.1959.8.698

624 16. Park SL, Huang Y-JS, Lyons AC, Ayers VB, Hettenbach SM, McVey DS, et al. North
625 American domestic pigs are susceptible to experimental infection with Japanese
626 encephalitis virus. Sci Rep. 2018;8: 7951. doi:10.1038/s41598-018-26208-8

627 17. Ricklin ME, García-Nicolás O, Brechbühl D, Python S, Zumkehr B, Nougairede A, et al.
628 Vector-free transmission and persistence of Japanese encephalitis virus in pigs. Nat
629 Commun. 2016;7: 10832. doi:10.1038/ncomms10832

630 18. Lyons AC, Huang Y-JS, Park SL, Ayers VB, Hettenbach SM, Higgs S, et al. Shedding
631 of Japanese Encephalitis Virus in Oral Fluid of Infected Swine. Vector-Borne and
632 Zoonotic Diseases. 2018;18: 469–474. doi:10.1089/vbz.2018.2283

633 19. Diallo AOI, Chevalier V, Cappelle J, Duong V, Fontenille D, Duboz R. How much does
634 direct transmission between pigs contribute to Japanese Encephalitis virus circulation?
635 A modelling approach in Cambodia. Munderloh UG, editor. PLoS ONE. 2018;13:
636 e0201209. doi:10.1371/journal.pone.0201209

637 20. Scherer WF, Moyer JT, Izumi T. Immunologic studies of Japanese encephalitis virus in
638 Japan. V. Maternal antibodies, antibody responses and viremia following infection of
639 swine. J Immunol. 1959;83: 620–626.

640 21. Cappelle J, Duong V, Pring L, Kong L, Yakovleff M, Prasetyo DB, et al. Intensive
641 Circulation of Japanese Encephalitis Virus in Peri-urban Sentinel Pigs near Phnom
642 Penh, Cambodia. Barrera R, editor. PLoS Negl Trop Dis. 2016;10: e0005149.
643 doi:10.1371/journal.pntd.0005149

644 22. Weaver SC, Reisen WK. Present and future arboviral threats. Antiviral Research.
645 2010;85: 328–345. doi:10.1016/j.antiviral.2009.10.008

646 23. Kraemer MUG, Reiner RC, Brady OJ, Messina JP, Gilbert M, Pigott DM, et al. Past and
647 future spread of the arbovirus vectors Aedes aegypti and Aedes albopictus. Nat
648 Microbiol. 2019;4: 854–863. doi:10.1038/s41564-019-0376-y

649 24. McGuinness SL, Lau CL, Leder K. The evolving Japanese encephalitis situation in
650 Australia and implications for travel medicine. Journal of Travel Medicine. 2023;30:
651 taad029. doi:10.1093/jtm/taad029

652 25. Seebach JD, Schneider MKJ, Comrack CA, LeGuern A, Kolb SA, Knolle PA, et al.
653 Immortalized bone-marrow derived pig endothelial cells: Immortalized pig endothelial
654 cells. Xenotransplantation. 2001;8: 48–61. doi:10.1034/j.1399-3089.2001.00075.x

655 26. Sautter CA, Trus I, Nauwynck H, Summerfield A. No Evidence for a Role for Antibodies
656 during Vaccination-Induced Enhancement of Porcine Reproductive and Respiratory
657 Syndrome. Viruses. 2019;11: 829. doi:10.3390/v11090829

658 27. Aubry F, Vongsouvath M, Nougairède A, Phetsouvanh R, Sibounheuang B, Charrel R,
659 et al. Complete Genome of a Genotype I Japanese Encephalitis Virus Isolated from a

660 Patient with Encephalitis in Vientiane, Lao PDR. Genome Announc. 2013;1.
661 doi:10.1128/genomeA.00157-12

662 28. Reed LJ, Muench H. A SIMPLE METHOD OF ESTIMATING FIFTY PER CENT
663 ENDPOINTS12. American Journal of Epidemiology. 1938;27: 493–497.
664 doi:10.1093/oxfordjournals.aje.a118408

665 29. Ricklin ME, Garcìa-Nicolàs O, Brechbühl D, Python S, Zumkehr B, Posthaus H, et al.
666 Japanese encephalitis virus tropism in experimentally infected pigs. Vet Res. 2016;47:
667 34. doi:10.1186/s13567-016-0319-z

668 30. Kim D, Pertea G, Trapnell C, Pimentel H, Kelley R, Salzberg SL. TopHat2: accurate
669 alignment of transcriptomes in the presence of insertions, deletions and gene fusions.
670 Genome Biol. 2013;14: R36. doi:10.1186/gb-2013-14-4-r36

671 31. Kim D, Salzberg SL. TopHat-Fusion: an algorithm for discovery of novel fusion
672 transcripts. Genome Biol. 2011;12: R72. doi:10.1186/gb-2011-12-8-r72

673 32. Trapnell C, Pachter L, Salzberg SL. TopHat: discovering splice junctions with RNA-Seq.
674 Bioinformatics. 2009;25: 1105–1111. doi:10.1093/bioinformatics/btp120

675 33. Langmead B, Trapnell C, Pop M, Salzberg SL. Ultrafast and memory-efficient alignment
676 of short DNA sequences to the human genome. Genome Biol. 2009;10: R25.
677 doi:10.1186/gb-2009-10-3-r25

678 34. Putri GH, Anders S, Pyl PT, Pimanda JE, Zanini F. Analysing high-throughput
679 sequencing data in Python with HTSeq 2.0. Boeva V, editor. Bioinformatics. 2022;38:
680 2943–2945. doi:10.1093/bioinformatics/btac166

681 35. Anders S, Pyl PT, Huber W. HTSeq—a Python framework to work with high-throughput
682 sequencing data. Bioinformatics. 2015;31: 166–169. doi:10.1093/bioinformatics/btu638

683 36. Love MI, Huber W, Anders S. Moderated estimation of fold change and dispersion for
684 RNA-seq data with DESeq2. Genome Biol. 2014;15: 550. doi:10.1186/s13059-014-
685 0550-8

686 37. Boccard J, Schvartz D, Codesido S, Hanafi M, Gagnebin Y, Ponte B, et al. Gaining
687 Insights Into Metabolic Networks Using Chemometrics and Bioinformatics: Chronic
688 Kidney Disease as a Clinical Model. Front Mol Biosci. 2021;8: 682559.
689 doi:10.3389/fmolb.2021.682559

690 38. Subramanian A, Tamayo P, Mootha VK, Mukherjee S, Ebert BL, Gillette MA, et al.
691 Gene set enrichment analysis: A knowledge-based approach for interpreting genome-
692 wide expression profiles. Proc Natl Acad Sci USA. 2005;102: 15545–15550.
693 doi:10.1073/pnas.0506580102

694 39. Benjamini Y, Hochberg Y. Controlling the False Discovery Rate: A Practical and
695 Powerful Approach to Multiple Testing. Journal of the Royal Statistical Society: Series B
696 (Methodological). 1995;57: 289–300. doi:10.1111/j.2517-6161.1995.tb02031.x

697 40. Li S, Rouphael N, Duraisingham S, Romero-Steiner S, Presnell S, Davis C, et al.
698 Molecular signatures of antibody responses derived from a systems biology study of
699 five human vaccines. Nat Immunol. 2014;15: 195–204. doi:10.1038/ni.2789

700 41. Matthijs AMF, Auray G, Jakob V, García-Nicolás O, Braun RO, Keller I, et al. Systems
701 Immunology Characterization of Novel Vaccine Formulations for Mycoplasma
702 hyopneumoniae Bacterins. Front Immunol. 2019;10: 1087.
703 doi:10.3389/fimmu.2019.01087

704 42. Guzylack-Piriou L, Balmelli C, McCullough KC, Summerfield A. Type-A CpG
705 oligonucleotides activate exclusively porcine natural interferon-producing cells to
706 secrete interferon-alpha, tumour necrosis factor-alpha and interleukin-12. Immunology.
707 2004;112: 28–37. doi:10.1111/j.1365-2567.2004.01856.x

708 43. Andrews S. A Quality Control Tool for High Throughput Sequence Data. 2022.
709 Available: http://www.bioinformatics.babraham.ac.uk/projects/fastqc/

710 44. Chen S, Zhou Y, Chen Y, Gu J. fastp: an ultra-fast all-in-one FASTQ preprocessor.
711 Bioinformatics. 2018;34: i884–i890. doi:10.1093/bioinformatics/bty560

712 45. Wood DE, Lu J, Langmead B. Improved metagenomic analysis with Kraken 2. Genome
713 Biol. 2019;20: 257. doi:10.1186/s13059-019-1891-0

714 46. Bankevich A, Nurk S, Antipov D, Gurevich AA, Dvorkin M, Kulikov AS, et al. SPAdes: A
715 New Genome Assembly Algorithm and Its Applications to Single-Cell Sequencing.
716 Journal of Computational Biology. 2012;19: 455–477. doi:10.1089/cmb.2012.0021

717 47. Li H. Aligning sequence reads, clone sequences and assembly contigs with BWA-MEM.
718 2013 [cited 30 Oct 2023]. doi:10.48550/ARXIV.1303.3997

719 48. Li H, Handsaker B, Wysoker A, Fennell T, Ruan J, Homer N, et al. The Sequence
720 Alignment/Map format and SAMtools. Bioinformatics. 2009;25: 2078–2079.
721 doi:10.1093/bioinformatics/btp352

722 49. Genomics, Fulcrum. Fgbio Tools. 2023. Available:
723 https://fulcrumgenomics.github.io/fgbio/tools/latest/.

724 50. McKenna A, Hanna M, Banks E, Sivachenko A, Cibulskis K, Kernytsky A, et al. The
725 Genome Analysis Toolkit: A MapReduce framework for analyzing next-generation DNA
726 sequencing data. Genome Res. 2010;20: 1297–1303. doi:10.1101/gr.107524.110

727 51. Wilm A, Aw PPK, Bertrand D, Yeo GHT, Ong SH, Wong CH, et al. LoFreq: a sequence-
728 quality aware, ultra-sensitive variant caller for uncovering cell-population heterogeneity
729 from high-throughput sequencing datasets. Nucleic Acids Research. 2012;40: 11189–
730 11201. doi:10.1093/nar/gks918

731 52. Pedersen BS, Quinlan AR. Mosdepth: quick coverage calculation for genomes and
732 exomes. Hancock J, editor. Bioinformatics. 2018;34: 867–868.
733 doi:10.1093/bioinformatics/btx699

734 53. Nelson CW, Moncla LH, Hughes AL. SNPGenie: estimating evolutionary parameters to
735 detect natural selection using pooled next-generation sequencing data. Bioinformatics.
736 2015;31: 3709–3711. doi:10.1093/bioinformatics/btv449

737 54. Shannon P, Markiel A, Ozier O, Baliga NS, Wang JT, Ramage D, et al. Cytoscape: A
738 Software Environment for Integrated Models of Biomolecular Interaction Networks.
739 Genome Res. 2003;13: 2498–2504. doi:10.1101/gr.1239303

740 55. R Core Team. R: A Language and Environment for Statistical Computing. 2022.
741 Available: https://www.R-project.org/.

742 56. Redant V, Favoreel HW, Dallmeier K, Van Campe W, De Regge N. Efficient control of
743 Japanese encephalitis virus in the central nervous system of infected pigs occurs in the
744 absence of a pronounced inflammatory immune response. J Neuroinflammation.
745 2020;17: 315. doi:10.1186/s12974-020-01974-3

746 57. Radulovic E, Mehinagic K, Wüthrich T, Hilty M, Posthaus H, Summerfield A, et al. The
747 baseline immunological and hygienic status of pigs impact disease severity of African
748 swine fever. Dixon LK, editor. PLoS Pathog. 2022;18: e1010522.
749 doi:10.1371/journal.ppat.1010522

750 58. Bocard LV, Kick AR, Hug C, Lischer HEL, Käser T, Summerfield A. Systems
751 Immunology Analyses Following Porcine Respiratory and Reproductive Syndrome Virus
752 Infection and Vaccination. Front Immunol. 2021;12: 779747.
753 doi:10.3389/fimmu.2021.779747

754 59. Weaver SC, Forrester NL, Liu J, Vasilakis N. Population bottlenecks and founder
755 effects: implications for mosquito-borne arboviral emergence. Nat Rev Microbiol.
756 2021;19: 184–195. doi:10.1038/s41579-020-00482-8

757 60. Domingo E, Holland JJ. RNA VIRUS MUTATIONS AND FITNESS FOR SURVIVAL.
758 Annu Rev Microbiol. 1997;51: 151–178. doi:10.1146/annurev.micro.51.1.151

759 61. Halabi K, Mayrose I. Mechanisms Underlying Host Range Variation in Flavivirus: From
760 Empirical Knowledge to Predictive Models. J Mol Evol. 2021;89: 329–340.
761 doi:10.1007/s00239-021-10013-5

762 62. Deardorff ER, Fitzpatrick KA, Jerzak GVS, Shi P-Y, Kramer LD, Ebel GD. West Nile
763 Virus Experimental Evolution in vivo and the Trade-off Hypothesis. Wilke CO, editor.
764 PLoS Pathog. 2011;7: e1002335. doi:10.1371/journal.ppat.1002335

765 63. Liu Z, Zhang Y, Cheng M, Ge N, Shu J, Xu Z, et al. A single nonsynonymous mutation
766 on ZIKV E protein-coding sequences leads to markedly increased neurovirulence in
767 vivo. Virologica Sinica. 2022;37: 115–126. doi:10.1016/j.virs.2022.01.021

768 64. Jaeger AS, Marano J, Riemersma KK, Castaneda D, Pritchard EM, Pritchard JC, et al.
769 Gain without pain: adaptation and increased virulence of Zika virus in vertebrate host
770 without fitness cost in mosquito vector. Lowen AC, editor. J Virol. 2023;97: e01162-23.
771 doi:10.1128/jvi.01162-23

772 65. Riemersma KK, Jaeger AS, Crooks CM, Braun KM, Weger-Lucarelli J, Ebel GD, et al.
773 Rapid Evolution of Enhanced Zika Virus Virulence during Direct Vertebrate
774 Transmission Chains. Parrish CR, editor. J Virol. 2021;95: e02218-20.
775 doi:10.1128/JVI.02218-20

776 66. Wu R, Tian Y, Deng J, Yang K, Liang W, Guo R, et al. Multiple amino acid variations in
777 the nonstructural proteins of swine Japanese encephalitis virus alter its virulence in
778 mice. Arch Virol. 2011;156: 685–688. doi:10.1007/s00705-010-0871-1

779 67. McCurdy K, Joyce J, Hamilton S, Nevins C, Sosna W, Puricelli K, et al. Differential
780 accumulation of genetic and phenotypic changes in Venezuelan equine encephalitis
781 virus and Japanese encephalitis virus following passage in vitro and in vivo. Virology.
782 2011;415: 20–29. doi:10.1016/j.virol.2011.03.030

783 68. Thompson PB. Swine care handbook. Indiana State Board of Animal Health; 2022 Mar.
784 Available: https://www.in.gov/boah/files/swinecarehandbook.pdf

785 69. Council of the European Union. Consolidated text: Council Directive 2008/120/EC of 18
786 December 2008 laying down minimum standards for the protection of pigs (Codified
787 version). Dec 14, 2019 pp. 5–13. Available: https://eur-lex.europa.eu/legal-
788 content/EN/ALL/?uri=CELEX:02008L0120-20191214

789 70. Victorian Standards and Guidelines for the Welfare of Pigs. Revision 1. Melbourne,
790 Victoria: Department of Primary Industries, Biosecurity Victoria; 2012.

791 71. Maes D, Deluyker H, Verdonck M, Castryck F, Miry C, Vrijens B, et al. Herd factors
792 associated with the seroprevalences of four major respiratory pathogens in slaughter
793 pigs from farrow-to-finish pig herds. Vet Res. 2000;31: 313–327.
794 doi:10.1051/vetres:2000122

795 72. Li X, Xiong X, Wu X, Liu G, Zhou K, Yin Y. Effects of stocking density on growth
796 performance, blood parameters and immunity of growing pigs. Animal Nutrition. 2020;6:
797 529–534. doi:10.1016/j.aninu.2020.04.001

798 73. Department of Agriculture, Fisheries and Forestry, Australian Government. Japanese
799 encephalitis virus. In: Australian Government [Internet]. 2023. Available:

https://www.agriculture.gov.au/biosecurity-trade/pests-diseases-weeds/animal/japanese-encephalitis

74. Mackenzie JS, Williams DT, Van Den Hurk AF, Smith DW, Currie BJ. Japanese Encephalitis Virus: The Emergence of Genotype IV in Australia and Its Potential Endemicity. Viruses. 2022;14: 2480. doi:10.3390/v14112480

75. Xu G, Gao T, Wang Z, Zhang J, Cui B, Shen X, et al. Re-Emerged Genotype IV of Japanese Encephalitis Virus Is the Youngest Virus in Evolution. Viruses. 2023;15: 626. doi:10.3390/v15030626

76. Ciota AT, Lovelace AO, Ngo KA, Le AN, Maffei JG, Franke MA, et al. Cell-specific adaptation of two flaviviruses following serial passage in mosquito cell culture. Virology. 2007;357: 165–174. doi:10.1016/j.virol.2006.08.005

77. Lee E, Hall RA, Lobigs M. Common E Protein Determinants for Attenuation of Glycosaminoglycan-Binding Variants of Japanese Encephalitis and West Nile Viruses. J Virol. 2004;78: 8271–8280. doi:10.1128/JVI.78.15.8271-8280.2004

78. Lee E, Lobigs M. Mechanism of Virulence Attenuation of Glycosaminoglycan-Binding Variants of Japanese Encephalitis Virus and Murray Valley Encephalitis Virus. J Virol. 2002;76: 4901–4911. doi:10.1128/JVI.76.10.4901-4911.2002

79. Sui L, Zhao Y, Wang W, Chi H, Tian T, Wu P, et al. Flavivirus prM interacts with MDA5 and MAVS to inhibit RLR antiviral signaling. Cell Biosci. 2023;13: 9. doi:10.1186/s13578-023-00957-0

80. He M-J, Wang H-J, Yan X-L, Lou Y-N, Song G-Y, Li R-T, et al. Key Residue in the Precursor Region of M Protein Contributes to the Neurovirulence and Neuroinvasiveness of the African Lineage of Zika Virus. Heise MT, editor. J Virol. 2023;97: e01801-22. doi:10.1128/jvi.01801-22

824 81. Kim J-M, Yun S-I, Song B-H, Hahn Y-S, Lee C-H, Oh H-W, et al. A Single N-Linked
825 Glycosylation Site in the Japanese Encephalitis Virus prM Protein Is Critical for Cell
826 Type-Specific prM Protein Biogenesis, Virus Particle Release, and Pathogenicity in
827 Mice. J Virol. 2008;82: 7846–7862. doi:10.1128/JVI.00789-08

828 82. Tajima S, Shibasaki K, Taniguchi S, Nakayama E, Maeki T, Lim C-K, et al. E and prM
829 proteins of genotype V Japanese encephalitis virus are required for its increased
830 virulence in mice. Heliyon. 2019;5: e02882. doi:10.1016/j.heliyon.2019.e02882

831 83. Kolodziejek J, Jungbauer C, Aberle SW, Allerberger F, Bagó Z, Camp JV, et al.
832 Integrated analysis of human-animal-vector surveillance: West Nile virus infections in
833 Austria, 2015–2016. Emerging Microbes & Infections. 2018;7: 1–15.
834 doi:10.1038/s41426-018-0021-5

835 84. Tsioka K, Gewehr S, Pappa S, Kalaitzopoulou S, Stoikou K, Mourelatos S, et al. West
836 Nile Virus in Culex Mosquitoes in Central Macedonia, Greece, 2022. Viruses. 2023;15:
837 224. doi:10.3390/v15010224

838 85. Li C, Bai X, Meng R, Shaozhou W, Zhang Q, Hua R, et al. Identification of a New
839 Broadly Cross-reactive Epitope within Domain III of the Duck Tembusu Virus E Protein.
840 Sci Rep. 2016;6: 36288. doi:10.1038/srep36288

841 86. Oude Munnink BB, Münger E, Nieuwenhuijse DF, Kohl R, Van Der Linden A,
842 Schapendonk CME, et al. Genomic monitoring to understand the emergence and
843 spread of Usutu virus in the Netherlands, 2016–2018. Sci Rep. 2020;10: 2798.
844 doi:10.1038/s41598-020-59692-y

845 87. Baillie GJ, Kolokotronis S-O, Waltari E, Maffei JG, Kramer LD, Perkins SL. Phylogenetic
846 and evolutionary analyses of St. Louis encephalitis virus genomes. Molecular
847 Phylogenetics and Evolution. 2008;47: 717–728. doi:10.1016/j.ympev.2008.02.015

848 88. Grard G, Moureau G, Charrel RN, Holmes EC, Gould EA, De Lamballerie X. Genomics
849 and evolution of Aedes-borne flaviviruses. Journal of General Virology. 2010;91: 87–94.
850 doi:10.1099/vir.0.014506-0

851 89. Soe AM, Ngwe Tun MM, Nabeshima T, Myat TW, Htun MM, Lin H, et al. Emergence of
852 a Novel Dengue Virus 3 (DENV-3) Genotype-I Coincident with Increased DENV-3
853 Cases in Yangon, Myanmar between 2017 and 2019. Viruses. 2021;13: 1152.
854 doi:10.3390/v13061152

855 90. Maruyama SR, Castro-Jorge LA, Ribeiro JMC, Gardinassi LG, Garcia GR, Brandão LG,
856 et al. Characterisation of divergent flavivirus NS3 and NS5 protein sequences detected
857 in Rhipicephalus microplus ticks from Brazil. Mem Inst Oswaldo Cruz. 2014;109: 38–50.
858 doi:10.1590/0074-0276130166

859 91. Ayub A, Ashfaq UA, Idrees S, Haque A. Global Consensus Sequence Development and
860 Analysis of Dengue NS3 Conserved Domains. BioResearch Open Access. 2013;2:
861 392–396. doi:10.1089/biores.2013.0022

862 92. Pan X-L, Liu H, Wang H-Y, Fu S-H, Liu H-Z, Zhang H-L, et al. Emergence of genotype I
863 of Japanese encephalitis virus as the dominant genotype in Asia. J Virol. 2011;85:
864 9847–9853. doi:10.1128/JVI.00825-11

865 93. Xiao C, Li C, Di D, Cappelle J, Liu L, Wang X, et al. Differential replication efficiencies
866 between Japanese encephalitis virus genotype I and III in avian cultured cells and
867 young domestic ducklings. Samy AM, editor. PLoS Negl Trop Dis. 2018;12: e0007046.
868 doi:10.1371/journal.pntd.0007046

869 94. Lu G, Gong P. Crystal Structure of the Full-Length Japanese Encephalitis Virus NS5
870 Reveals a Conserved Methyltransferase-Polymerase Interface. Tellinghuisen TL, editor.
871 PLoS Pathog. 2013;9: e1003549. doi:10.1371/journal.ppat.1003549

872 95. Wu J, Lu G, Zhang B, Gong P. Perturbation in the Conserved Methyltransferase-
873 Polymerase Interface of Flavivirus NS5 Differentially Affects Polymerase Initiation and
874 Elongation. Perlman S, editor. J Virol. 2015;89: 249–261. doi:10.1128/JVI.02085-14

875 96. Ballesteros JA, Deupi X, Olivella M, Haaksma EEJ, Pardo L. Serine and Threonine
876 Residues Bend α-Helices in the χ1=g− Conformation. Biophysical Journal. 2000;79:
877 2754–2760. doi:10.1016/S0006-3495(00)76514-3

878 97. Papageorgiou L, Loukatou S, Sofia K, Maroulis D, Vlachakis D. An updated
879 evolutionary study of Flaviviridae NS3 helicase and NS5 RNA-dependent RNA
880 polymerase reveals novel invariable motifs as potential pharmacological targets. Mol
881 BioSyst. 2016;12: 2080–2093. doi:10.1039/C5MB00706B

882 98. Dubankova A, Boura E. Structure of the yellow fever NS5 protein reveals conserved
883 drug targets shared among flaviviruses. Antiviral Research. 2019;169: 104536.
884 doi:10.1016/j.antiviral.2019.104536

885

886 **Figures and figure captions:**

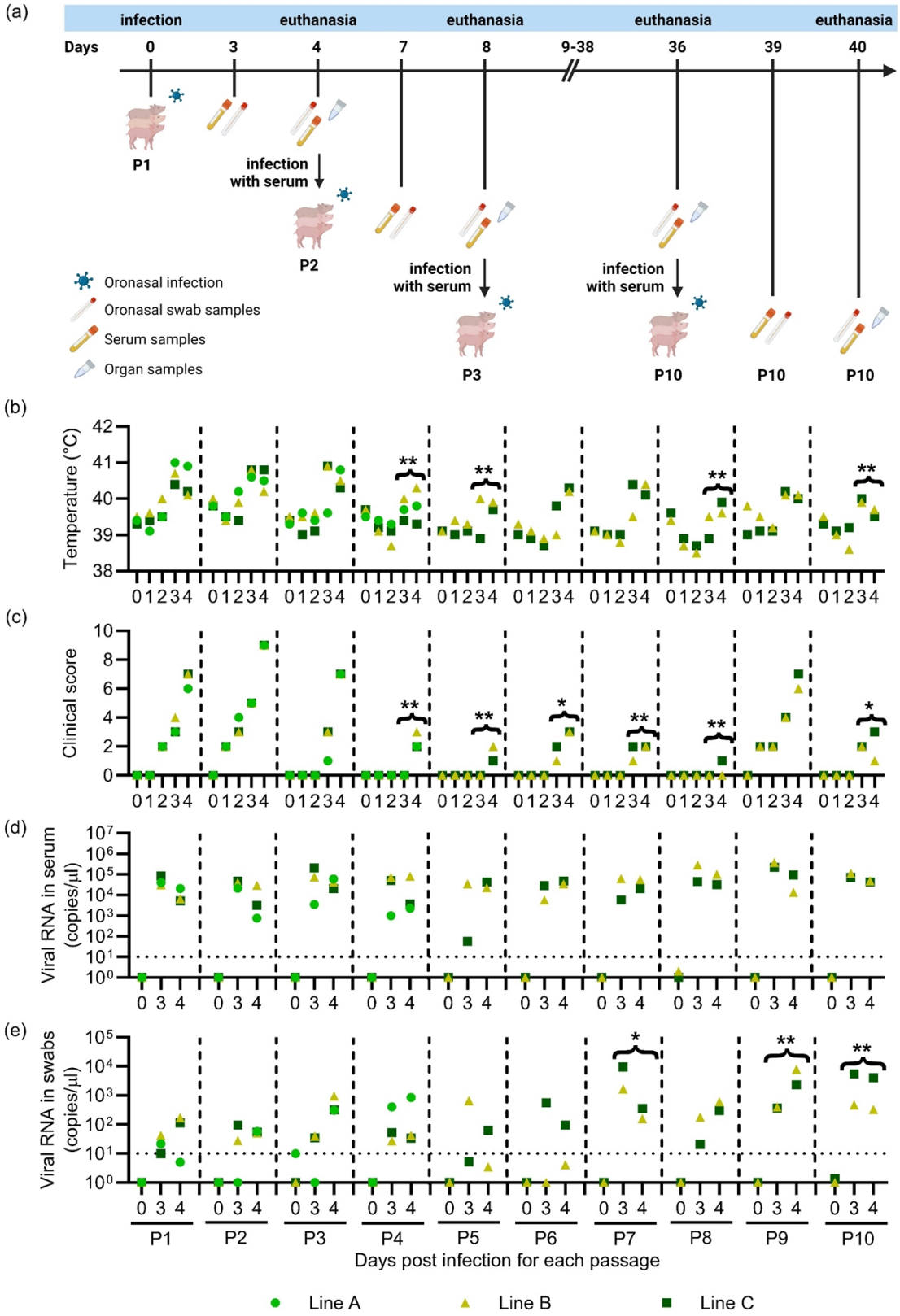


887

888 **Fig 1. Serial passaging of JEV in pigs.** In (a), the experimental layout and sampling time
889 points are schematically represented (graphic created with BioRender.com). The passaging
890 was performed in three independent lines A-C. For P1, three pigs were oro-nasally infected
891 with JEV P0. To generate P2-P10, pigs were oro-nasally infected with serum collected at four
892 days post-infection of the previous passages. Line A was lost after P4. In (b)-(e), body
893 temperatures, clinical scores, viral RNA loads in serum and in oro-nasal swabs are shown,
894 respectively. The clinical scores were determined following a clinical score sheet
895 (Supplementary methods). The temperature, clinical score and viral RNA load values of day
896 3 and 4 of each passage were combined (represented by braces) to enable statistical
897 analysis. All combined values were compared to the corresponding P1 values using Mann-
898 Whitney U tests (*p<0.05, **p<0.01; ***p<0.001; **** p<0.0001).

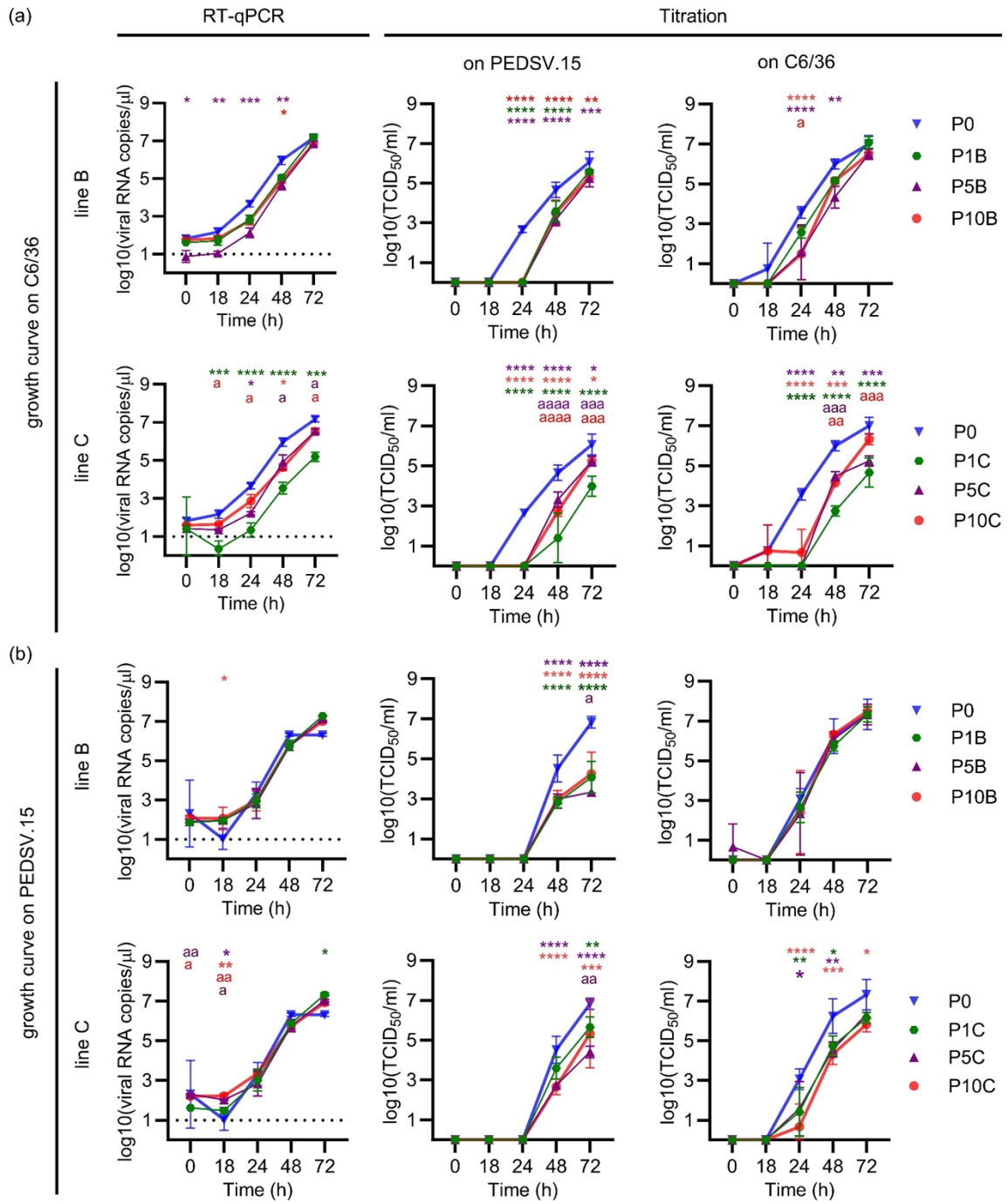


899

900 **Fig 2. *In vitro* growth curves of passaged JEV.** The insect cells C6/36 (a) or the porcine
901 cell line PEDSV.15 (b) were infected with a MOI of 0.01 $TCID_{50}$/cell with P0 (blue), P1
902 (green), P5 (purple) or P10 (red) in triplicates. Passage lines B and C were depicted
903 separately. The presence of the virus was analysed by RT-qPCR, as well as by titration on
904 C6/36 and PEDSV.15 cells. Statistical significance was determined using Tukey's multiple

905 comparison test (ANOVA) using either the P0 values as reference (*p<0.05, **p<0.01;
906 ***p<0.001; ****p<0.0001) or following exclusion of P0 using the P1 values as reference
907 ([a]p<0.05, [aa]p<0.01; [aaa]p<0.001; [aaaa] p<0.0001). The same colour code as above was used to
908 indicate the affiliated groups.

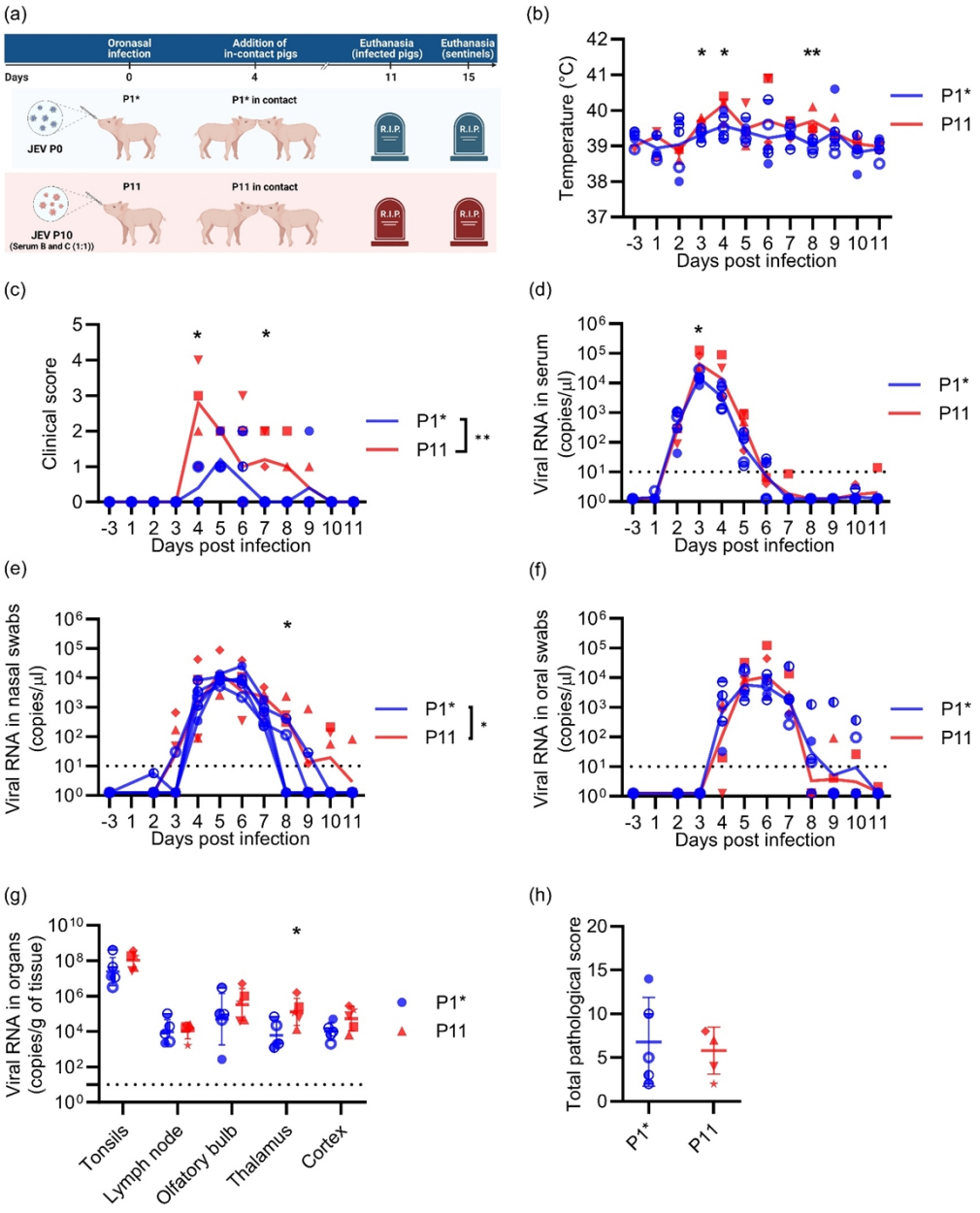


909

910 **Fig 3. *In vivo* characterization of passaged JEV – clinical, virological and pathological**
911 **data.** In (a) a schematic representation of the animal experiment is shown (created with

BioRender.com). Five pigs were oro-nasally infected with JEV P0 and five pigs with P10. The pigs infected with JEV P0 were labelled as P1* to differentiate from the first animal experiment, while the group infected with the mixture of P10 serum was termed P11. At 4 dpi, four naïve non-infected pigs were added to each group to determine direct transmission event. In (b)-(h), data from the oro-nasally infected pigs is shown, including body temperature (b), clinical scores (c) serum viral RNA loads (d), viral RNA loads in nasal swabs (e), viral RNA loads in oral swabs (f), viral RNA loads in CNS and lymphoid tissue (g) and histopathological scores of CNS tissues (h). This score represents additive data from 10 brain tissue samples (details in Supplementary Fig 2). Statistical analyses used the Mann-Whitney U test, comparing the P0 to P10 values at each time point. In addition, in (b) to (f), the area under the curve was compared between the two groups, using unpaired t-tests (indicated in the legends of the panels). The significance levels for both tests are indicated as *p<0.05, **p<0.01; ***p<0.001; ****<0.0001.

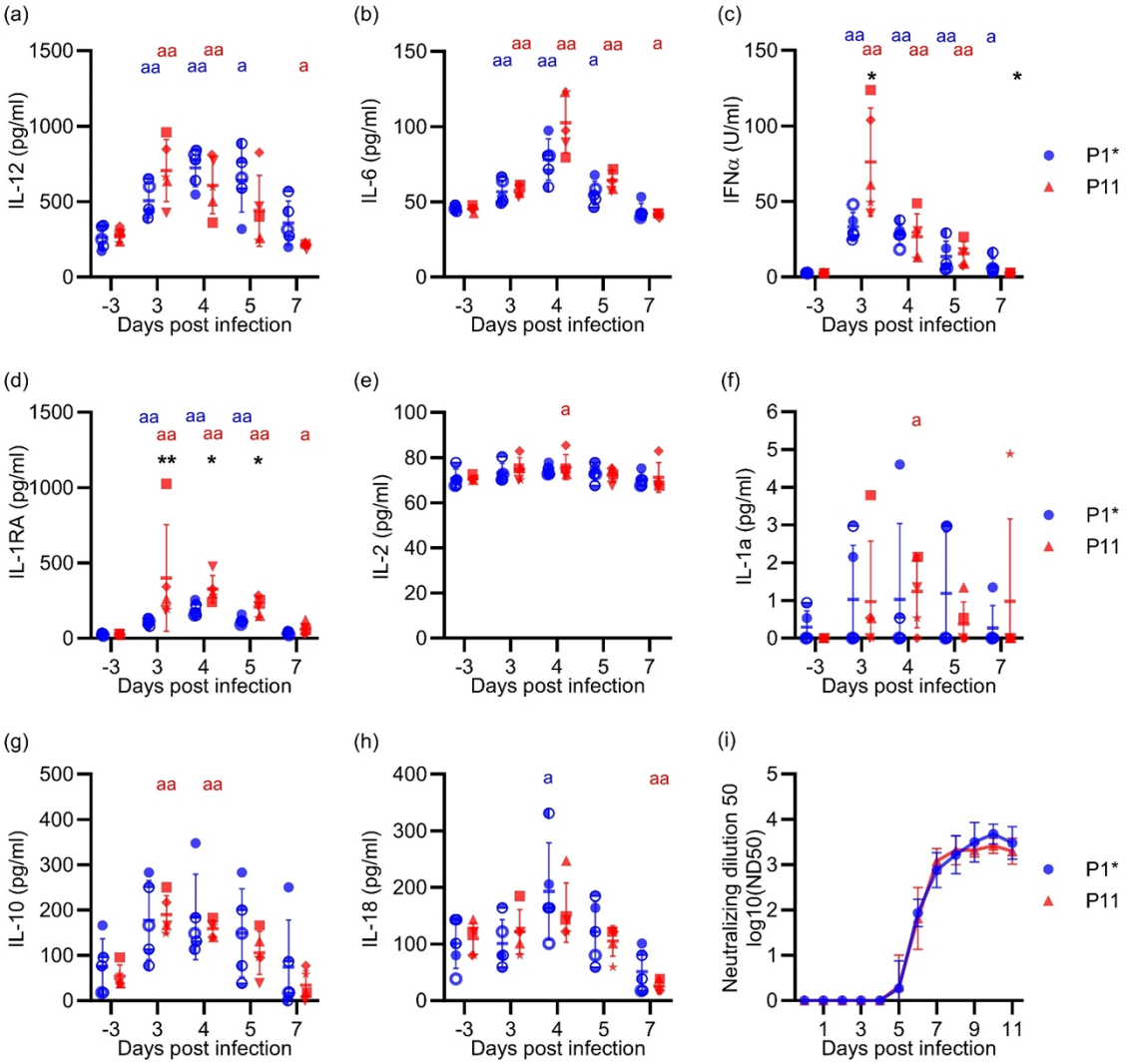


925

926 **Fig 4. Cytokines and neutralizing antibodies in the serum of JEV-infected pigs.** Sera
927 from the animal experiment schematically represented in Fig 3a was analysed. Panels (a-h)
928 show the levels of IL-12, IL-6, IFN-α, IL-1RA, IL-2, IL-1a, IL-10 and IL-18, respectively. Panel
929 (i) displays the levels of neutralising. The statistically significant differences between groups
930 on the same day are depicted as an asterisk, whereas differences compared to day -3 within
931 the same group is depicted by the letter "a". All statistical analyses were done using the
932 Mann-Whitney U test ($^{a/}$*p<0.05, $^{aa/}$**p<0.01; $^{aaa/}$***p<0.001; $^{aaaa/}$****<0.0001).

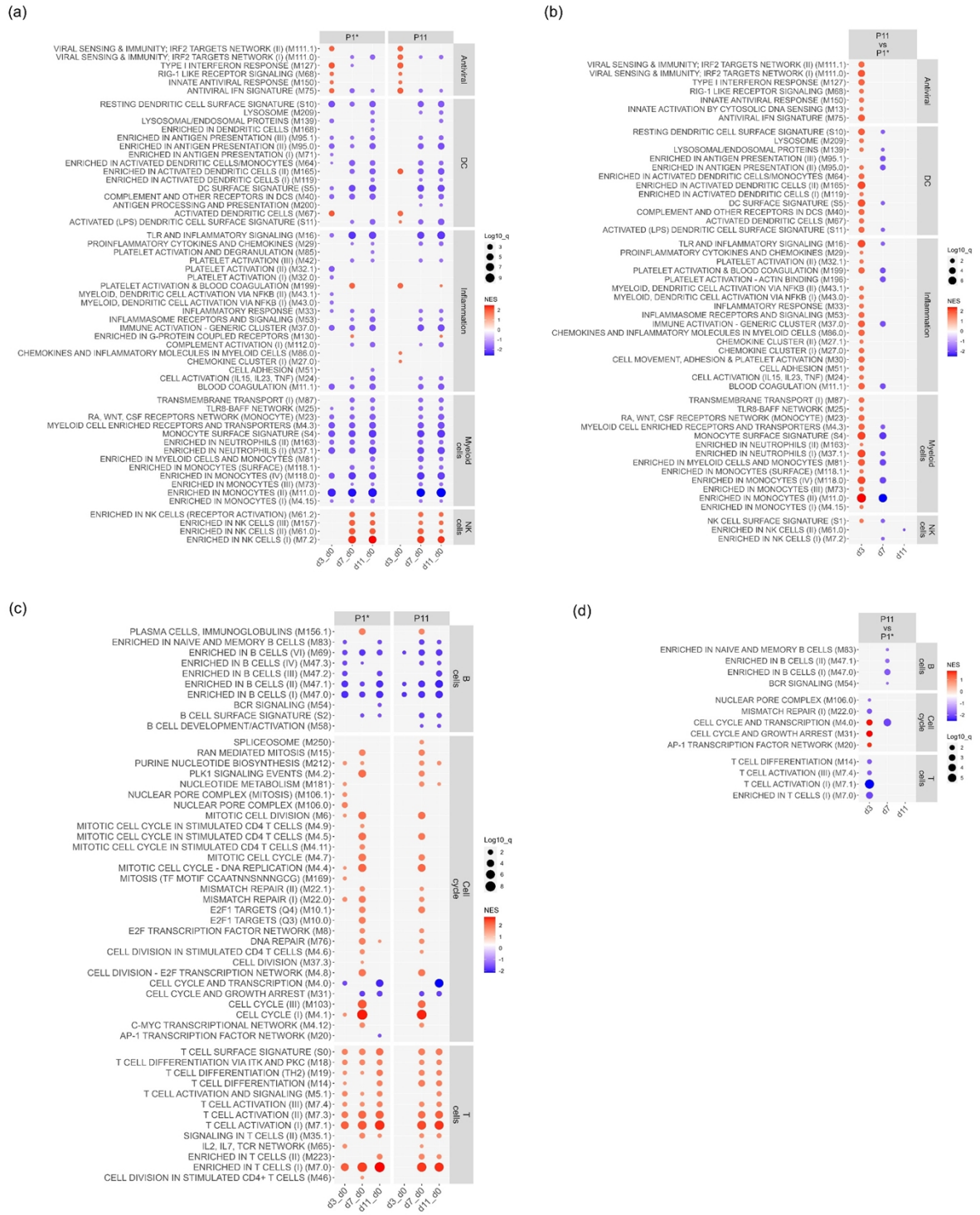


933

934 **Fig 5. Transcriptomic profiles leukocytes of the P1* and P11 groups**. Blood leukocytes

935 from uninfected, and JEV-infected at 3, 7 and 11 dpi of the P0/P10 *in vivo* characterization

936 experiment (Fig 3a) were subjected to mRNA sequencing and analysed by GSEA using

937 porcine BTM gene sets. The dot plots show the normalised enrichment scores (NES; red

upregulated, blue downregulated) with q-values indicated by dot sizes (cut-off at 0.05). The innate BTM gene sets (left y-axis labels) shown in (a) and (b) were further classified as "antiviral", "DC", "inflammation", myeloid cells", and "NK cells" (right y-axis label). The adaptive BTM shown in (c) and (d) were classified as "B cells", "cell cycle", and "T cells". In (a, c), the timepoints of infected pigs (n=5) were compared to uninfected pigs ("d0"), using the same baseline for the two groups. In (b, d), a comparison of JEV P10 (P11 group) versus P0 (P1* group) on different dpi is shown.

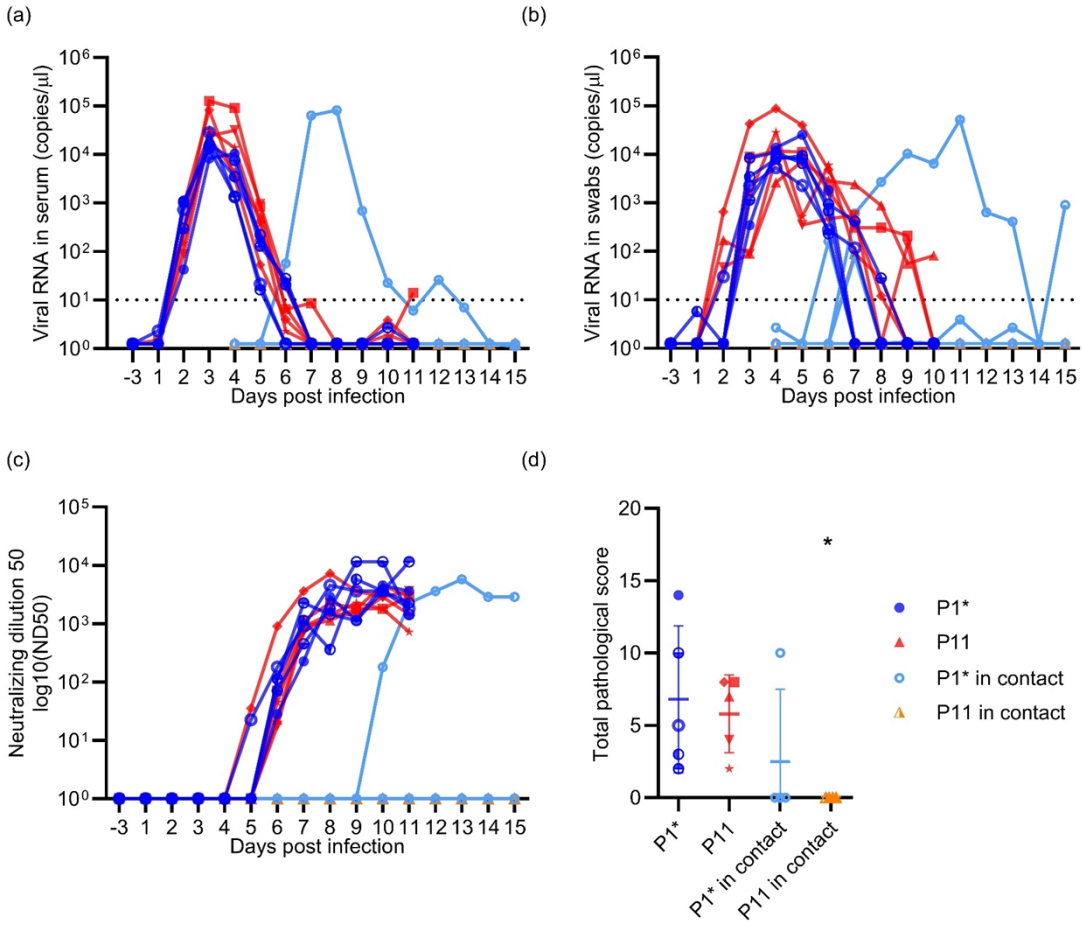


**Fig 6. Direct transmission of JEV between pigs.** Five pigs were oro-nasally infected with JEV P0 (P1* group) and five pigs with JEV P10 (P11 group). At four days post-infection, four pigs were added to each group to determine a possible direct transmission. In (a) and (b), viral RNA loads in the serum and nasal swabs are shown, respectively. Only one of the total

950 eight sentinels (light blue line, in contact with the P1* pigs) got viremic (a) and positive for
951 viral RNA in oro-nasal swabs (b). In (c), the neutralising antibody titres are shown, and in (d),
952 the pathological lesion scores in the CNS.

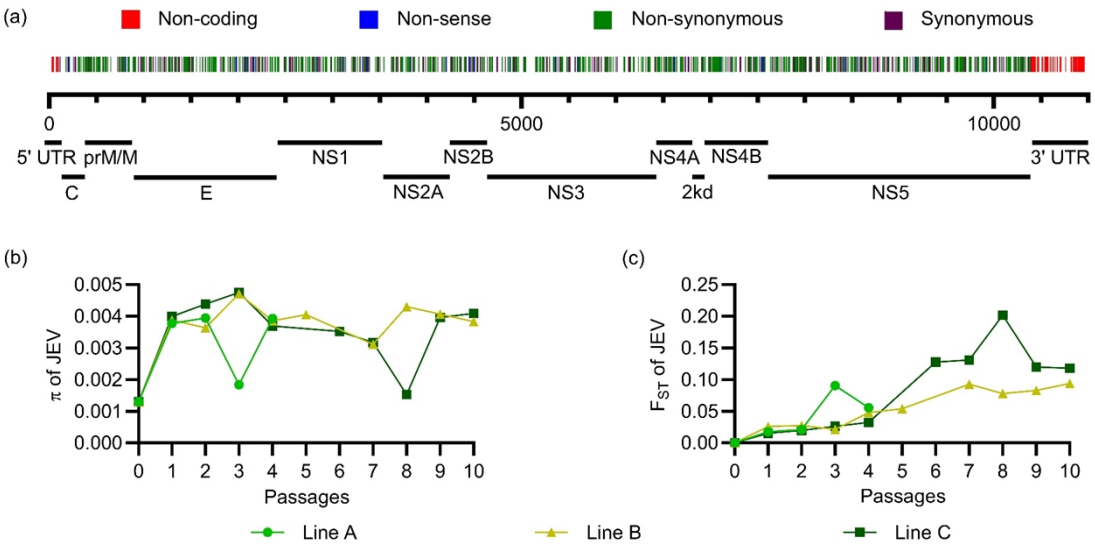


953

954 **Fig 7. Genomic changes during passaging.** In (a), the single-nucleotide variants found in
955 all passages across the genome are shown. Mutations in the UTR regions are depicted in
956 red; those leading to stop codons in blue (non-sense), non-synonymous mutations in green
957 and synonymous mutations in purple. In (b), the nucleotide diversity π calculated across the
958 whole genome is shown. In (c), the pairwise genetic differentiation between viral populations
959 in P0 and each passage is shown as fixation index $F_{ST}$, wherein 0 means no genetic
960 differentiation and 1 complete genetic differentiation. In (b) and (c), each line of passaging is
961 shown separately.

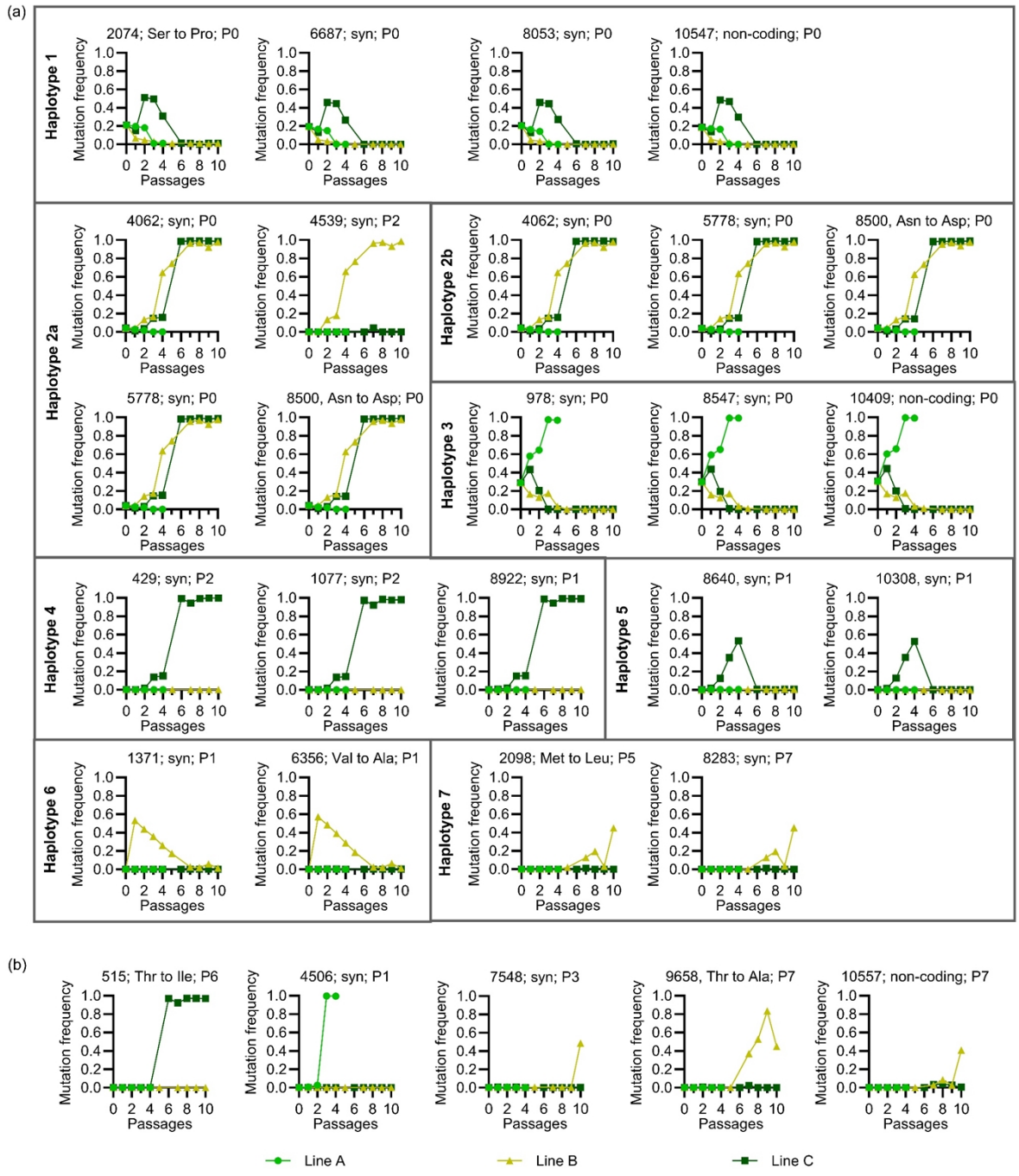


962

963 **Fig 8. Trajectory analyses of viral haplotypes and mutations.** Viral RNA was extracted
964 from the serum on 3 dpi and analysed by next-generation sequencing. Only mutations were
965 considered where an allele different from the major allele in P0 reached a frequency of at
966 least 35% in one of the passages. In (a), the mutations were grouped in different haplotypes
967 that followed quasi-identical allele frequency trajectories along the passages. These were

968 defined when a cosine similarity between the trajectories of nucleotide mutations in the
969 haplotype was > 0.999 for any comparison in that haplotype. In (b), individual mutations that
970 did not cluster in haplotypes are shown. For all plots, the position of the mutation, its impact
971 on the protein sequence with syn standing for synonymous mutation and the passage
972 number of the first detection of the mutation is shown.

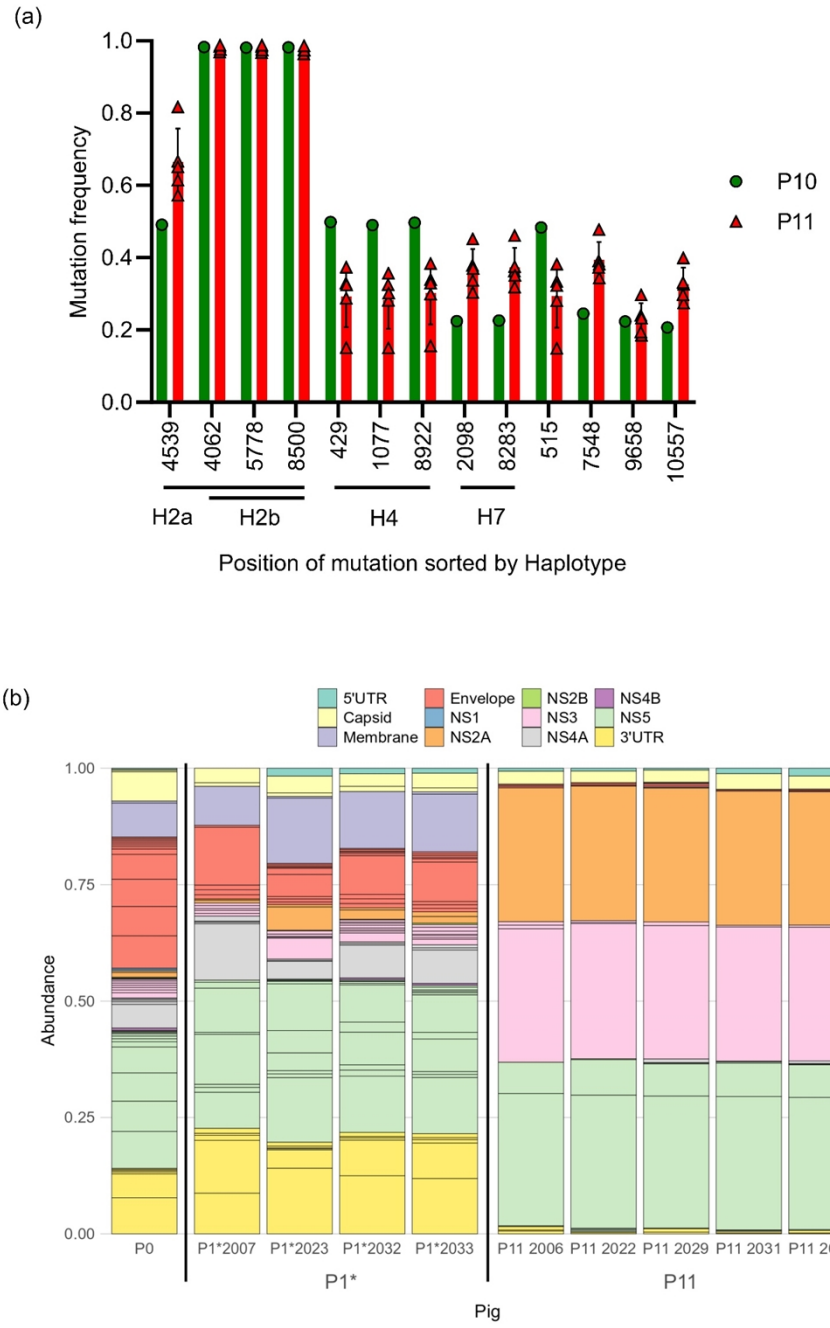


973

**Fig 9. Selection of haplotypes and divergent nucleotides during passaging.** JEV was passaged *in vivo* 10 times, resulting in P10 infectious serum. To check possible viral adaptations the P10 serum of lines B and C was used to further infect five pigs, resulting in P11. P11 was compared to a group of five pigs, infected with P0 (resulting in P1*). Serum samples were collected at 3 dpi for next-generation sequencing analyses. (a) Haplotypes and divergent nucleotides frequencies of input (P10, green) and output JEV (P11, red) are shown. For P10 the average frequencies of line P10B and P10C was calculated. For P11 each pig was depicted separately, with n=5 (symbols), while the bars represented the average frequencies. Only nucleotide changes reaching at least 35% in frequency are shown. (b) All nucleotide positions of P0 divergent from the JEV Laos reference genome were selected and the frequencies in P0, P1* and in P11 were plotted to visualize major positive and negative selections.

## Supporting information captions

**S1 Methods: Internal risk-benefit evaluation**

**S2 Methods: Clinical scores**

**S3 Methods: Cell culture media**

**S4 Methods: Construction of JEV RNA for quantitative RT-PCR**

**S5 Methods: Transcriptomics**

**S6 Methods: Histopathology**

**S7 Methods: Serum neutralisation assay**

**S8 Methods: Virus isolation from sera**

**S9 Methods: Virus sequencing**

**S1 Fig: Tissue distribution of JEV RNA during passaging.** In (a)-(e) RNA loads in tissues of the olfactory bulb, the cortex, the thalamus, the mandibular lymph nodes and the tonsils, respectively, are shown. For statistical analyses the values of the passages were compared

to the corresponding P1 values using Mann-Whitney U tests. No statistically significant differences ($p<0.05$) were identified.

**S2 Fig: Histopathological analyses of CNS from JEV infected pigs.** Formalin-fixed sections of the olfactory bulb (a), the rostral frontal cortex (b), the basal nuclei (c), the parietal cortex (d), the thalamus/ hippocampus (e), the cortex level of thalamus/ hippocampus (f), the occipital cortex (g), the midbrain (h), the cerebellum (i), the brain stem (j) and the spinal cord cervical (k) were embedded in paraffin, cut at 4 µm and HE-stained. Lesions were semi-quantitatively scored from 0 to 3 (0 = no lesions, 1 = mild, 2 = lesions, and 3 = severe lesions). For the cervical spinal cord the P10 group is missing two samples. Statistical analysis were performed using Mann-Whitney U test . The significance cut-off was set at $p <0.05$.

**S3 Fig: Unmodulated or undetectable cytokines in the serum of JEV-infected pigs.** Data for TNF (a), IL-8 (b), IL-4 (c) GM-CSF (d) and IL-1β (e) are shown. Statistical analysis was performed with Mann-Whitney U test. No significant increases in cytokine production ($p<0.05$) were found.

**S4 Fig: Nucleotide diversity π and fixation index $F_{ST}$ for individual viral genes and UTRs.** Viral RNA of d3 post-infection was analysed by next generation sequencing. For each viral gene and the UTRs, the nucleotide diversity π (plots on the left), and the pairwise genetic differentiation between viral populations in P0 and each passage is shown as fixation index $F_{ST}$ (plots on the right).

**S1 Table: Viral mutations and frequencies within each passage**

**S2 Table: Nucleotide diversity π and fixation index $F_{ST}$ for each passage**